Diego, CA, USA); anti-CD19-FITC, anti-CCR7-PE-Cy7 (BD Pharmingen, San Diego, CA, USA); anti-CD3-peridinin chlorophyll protein (PerCP), anti-CD8-APC-Cy7, anti-CD14-FITC (BD Biosciences, San Jose, CA, USA); and anti-CD56-FITC (eBioscience, San Diego, CA, USA). In the present study, lineage antigen (CD4, CD14, CD16, CD19, and CD56)-negative, CD3-, CD8-, and $WT1_{126}$ tetramer-positive lymphocytes were defined as $WT1_{126}$ tetramer$^+$ CD8$^+$ T cells. The $WT1_{126}$ tetramer$^+$ CD8$^+$ T cells were single-cell sorted using a FACSAria instrument (BD Biosciences), and data were analyzed using FACSDiva software (BD Biosciences).

Synthesis of cDNA from a single cell-sorted $WT1_{126}$ tetramer$^+$ CD8$^+$ T cell and determination of TCR-BV gene families. The $WT1_{126}$ tetramer$^+$ CD8$^+$ T cells were directly single-cell sorted into PCR tubes containing cDNA reaction mix, and cDNA synthesis was performed as described previously.[30] The cDNA was amplified using 24 kinds of TCR-BV gene family-specific forward primers and a constant region-specific reverse primer.[30] Next, the PCR products were amplified by semi-nested PCR for the screening of the BV gene family as follows: the first PCR product was put into eight separate tubes, each of which was filled with a reaction mix containing the reagents, one of eight kinds of screening sets of BV gene family-specific forward primers and the reverse primer. The eight kinds of screening sets used in the present study were the same as those used in a previous study.[30] Each screening PCR product was run on a 2% agarose gel to identify the positive reaction among the eight kinds of screening sets. Finally, the TCR-BV gene family was identified by the second round of PCR using an individual TCR-BV gene family-specific forward primer, which was contained in the positive screening set, and the reverse primer. As a negative control, three PCR tubes without sorted cells were prepared in each experiment and were subjected to the same RT-PCR procedures.

A total of 750 $WT1_{126}$ tetramer$^+$ CD8$^+$ T cells were analyzed in six patients (i.e. 59, 66, 46, 67, 88, and 73 cells from PT-1, -2, -3, -4, -5, and -6, respectively) and five HDs (i.e. 53, 57, 77, 79, and 85 cells from HD-1, -2, -3, -4, and -5, respectively). The International Immunogenetics Information System (IMGT) database site (http://www.imgt.org/IMGT_vquest/vquest?livret=0&Option=humanTcR, accessed 15 Nov 2011) was used to identify the human TCR-BV gene family.

Statistical analysis. The Mann–Whitney *U*-test was used to evaluate differences in frequencies and subset compositions of $WT1_{126}$ tetramer$^+$ CD8$^+$ T cells and CD3$^+$ CD8$^+$ T cells between patients and HDs. The significance of differences in usage frequencies of the 24 kinds of BV gene families between patients and HDs was also assessed using the Mann–Whitney *U*-test. Analyses were performed with the Stat Flex statistical software package (Artech, Osaka, Japan).

Results

Increase in $WT1_{126}$ tetramer$^+$ CD8$^+$ T cells with effector memory phenotype in HLA-A*0201$^+$ patients with solid tumors. The CTL responses to an HLA-A*0201-restricted epitope $WT1_{126}$ of the WT1 protein were examined in HLA-A*0201$^+$ patients with solid tumors. The PBMC were FACS analyzed by using $WT1_{126}$ tetramer (Fig. 1), with Figure 1(a) showing representative profiles of the FACS analysis of $WT1_{126}$ tetramer$^+$ CD8$^+$ T cells. The frequencies of $WT1_{126}$ tetramer$^+$ CD8$^+$ T cells in patients and HDs were 0.007–0.122% (median 0.039%) and 0.009–0.079% (median 0.016%), respectively. Although there was a tendency for higher frequencies in patients than in HDs, the differences failed to reach statistical significance (data not shown).

Human CD3$^+$ CD8$^+$ T cells can be divided into four distinct differentiation stages according to the cell surface expression of CCR7 and CD45RA as follows: (i) CCR7$^+$ CD45RA$^+$ (naïve) cells; (ii) CCR7$^+$ CD45RA$^-$ (central memory) cells; (iii) CCR7$^-$ CD45RA$^-$ (effector memory) cells; and (iv) CCR7$^-$ CD45RA$^+$ (effector) cells.[32,33] These cell surface markers were used to classify the differentiation stages of $WT1_{126}$ tetramer$^+$ CD8$^+$ T cells and a representative pattern from PT-3 is shown in Figure 1(b). The frequency of the naïve phenotype of $WT1_{126}$ tetramer$^+$ CD8$^+$ T cells was significantly higher in HDs than in patients (45.8–68.4% [median 55.6%] *vs* 3.4–37.9% [median 19.9%], respectively; $P < 0.01$), while the frequency of the effector memory phenotype of $WT1_{126}$ tetramer$^+$ CD8$^+$ T cells was significantly higher in patients than in HDs (30.3–58.6% [median 49.0%] *vs* 15.8–34.4% [median 20.7%], respectively; $P < 0.01$; Fig. 1c). In contrast, there were no significant differences in frequencies of the four subsets of the whole CD3$^+$ CD8$^+$ T cells between patients and HDs (data not shown),

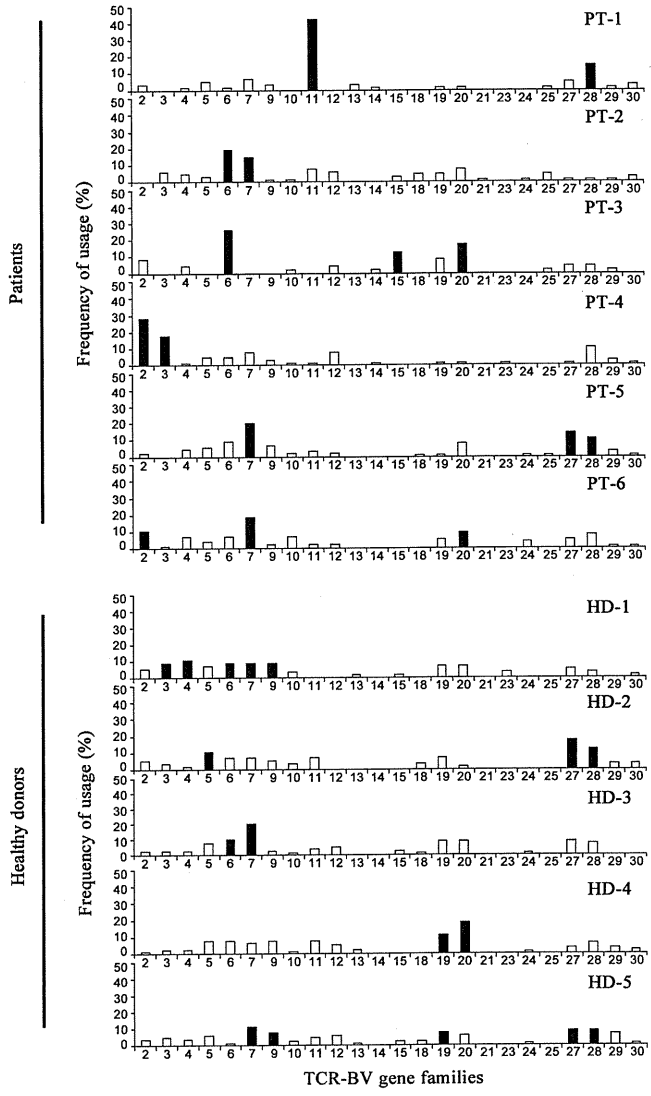

Fig. 2. Frequencies of T cell receptor β-chain variable region (TCR-BV) gene families used by T cell receptors (TCRs) in $WT1_{126}$ tetramer$^+$ CD8$^+$ T cells. The usage frequencies were defined as the ratio of (the number of a given TCR-BV gene family used)/(the total number of $WT1_{126}$ tetramer$^+$ CD8$^+$ T cells analyzed). Closed columns indicate that the usage frequency is higher than the mean value + 1SD.

doi: 10.1111/j.1349-7006.2011.02163.x

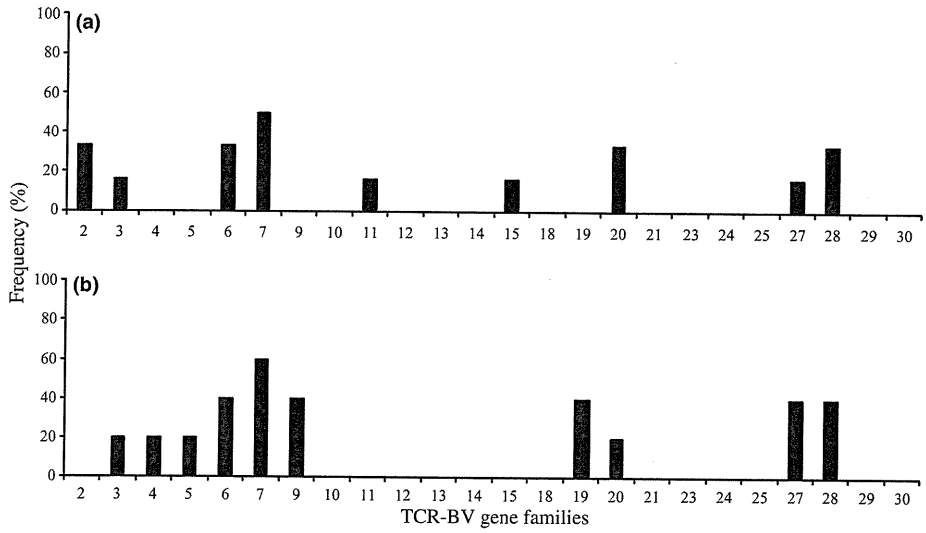

Fig. 3. Usage frequencies of T cell receptor β-chain variable region (TCR-BV) gene families with biased usage in (a) patients and (b) healthy donors. The ratios show the number of patients or healthy donors with biased usage of the specific TCR-BV gene families to the total number of patients or healthy donors examined, respectively.

indicating that the phenotypic difference in $CD3^+$ $CD8^+$ T cells between patients and HDs was restricted to $WT1_{126}$ tetramer$^+$ $CD8^+$ T cells. These results demonstrate that $WT1_{126}$ tetramer$^+$ $CD8^+$ T cells exhibit more differentiated/activated phenotypes in patients than in HDs.

Biased usage of TCR-BV gene families in $WT1_{126}$ tetramer$^+$ $CD8^+$ T cells. In the present study, TCR-BV gene families in $WT1_{126}$ tetramer$^+$ $CD8^+$ T cells were investigated by using the single cell-based RT-PCR technique for the six patients and five HDs. Usage frequencies for a given BV gene family were defined as the ratio of the number of $WT1_{126}$ tetramer$^+$ $CD8^+$ T cells with the usage of the BV gene family to the total number of $WT1_{126}$ tetramer$^+$ $CD8^+$ T cells analyzed. When the usage frequency of a given BV gene family was more than the mean value + 1SD for the usage of 24 different kinds of BV gene families, the usage was defined as biased, as described previously.[30] As shown in Figure 2, the biased usage of the TCR-BV gene families was as follows: BV2, in two of six patients; BV3, in one of six patients and one of five HDs; BV4, in one of five HDs; BV5, in one of five HDs; BV6, in two of six patients and two of five HDs; BV7, in three of six patients and three of five HDs; BV9, in two of five HDs; BV11, in one of six patients; BV15, in one of six patients; BV19, in two of five HDs; BV20, in two of six patients and one of five HDs; BV27, in one of six patients and two of five HDs; and BV28, in two of six patients and two of five HDs.

The ratios of the number of patients or HDs with biased usage of individual TCR-BV gene families in $WT1_{126}$ tetramer$^+$ $CD8^+$ T cells to the number of patients or HDs studied are shown in Figure 3. Nine TCR-BV gene families with biased usage were detected in patients and 10 were detected in HDs. These results show that: (i) BVs 3, 6, 7, 20, 27, and 28 are commonly biased in patients and HDs; (ii) BVs 2, 11, and 15 are biased only in patients; and (iii) BVs 4, 5, 9, and 19 are biased only in HDs.

The usage frequencies of TCR-BV gene families in patients reflect those in HDs. The frequencies of 24 TCR-BV gene families used by T cell receptors (TCRs) of $WT1_{126}$ tetramer$^+$ $CD8^+$ T cells were compared statistically between HLA-A*0201$^+$ patients and HDs (Fig. 4). In all BV gene families, except BVs 5 and 19, the usage frequencies did not differ significantly between patients and HDs, although the subset compositions of $WT1_{126}$ tetramer$^+$ $CD8^+$ T cells were significantly different between the two groups (see Fig. 1c). These results strongly indicate that the frequencies of TCR-BV families used by the TCR of $WT1_{126}$ tetramer$^+$ $CD8^+$ T cells in patients with solid tumors reflect those in HDs.

Discussion

Ratios of $WT1_{126}$ tetramer$^+$ $CD8^+$ T cells with the effector memory phenotype were significantly higher in HLA-A*0201$^+$ patients with solid tumors than in HLA-A*0201$^+$ HDs, while those with the naïve phenotype were significantly lower in patients than in HDs, indicating that $WT1_{126}$ tetramer$^+$ $CD8^+$ T cells were more activated and mature in patients than in HDs. These results are basically compatible with those of our previous study of $WT1_{235}$ tetramer$^+$ $CD8^+$ T cells in HLA-A*2402$^+$ patients with myeloid malignancies and HLA-A*2402$^+$ HDs, where the frequencies of $WT1_{235}$ tetramer$^+$ $CD8^+$ T cells were higher in patients than in HDs and $WT1_{235}$ tetramer$^+$ $CD8^+$ T cells were more activated and mature in patients than in HDs.[30]

In order to analyze TCR-BV gene family usage of the TCRs of human tumor-associated antigen (TAA)-reactive T cells, two methods are routinely used: (i) bulky lymphocyte populations are FACS analyzed using a panel of mAbs directed against individual TCR-BV gene family products; or (ii) the populations are analyzed by PCR using a panel of TCR-BV gene family-specific primers.[34–40] However, the former method does not cover all the BV gene segments distributed in each BV gene family and the latter does not guarantee that all the TCR-BV gene families are amplified from the cDNA with equal efficiency. For example, TCR-BV gene families of T cells that exist at very low frequencies in lymphocytes are easily missed using this sort of PCR method.[40] In contrast, because the present study was performed at the single cell level and because the amplification efficiency of TCR-BV cDNA from a single $WT1_{126}$ tetramer$^+$ $CD8^+$ T cell was >80% (data not shown), our results are thought to directly reflect TCR-BV gene family usage in $WT1_{126}$ tetramer$^+$ $CD8^+$ T cells.

Regardless of a striking difference in WT1-specific CTL responses between patients and HDs, the usage patterns of TCR-BV gene families in patients were similar to those in HDs. That is, patients and HDs shared biased usage of TCR-BV families 3,

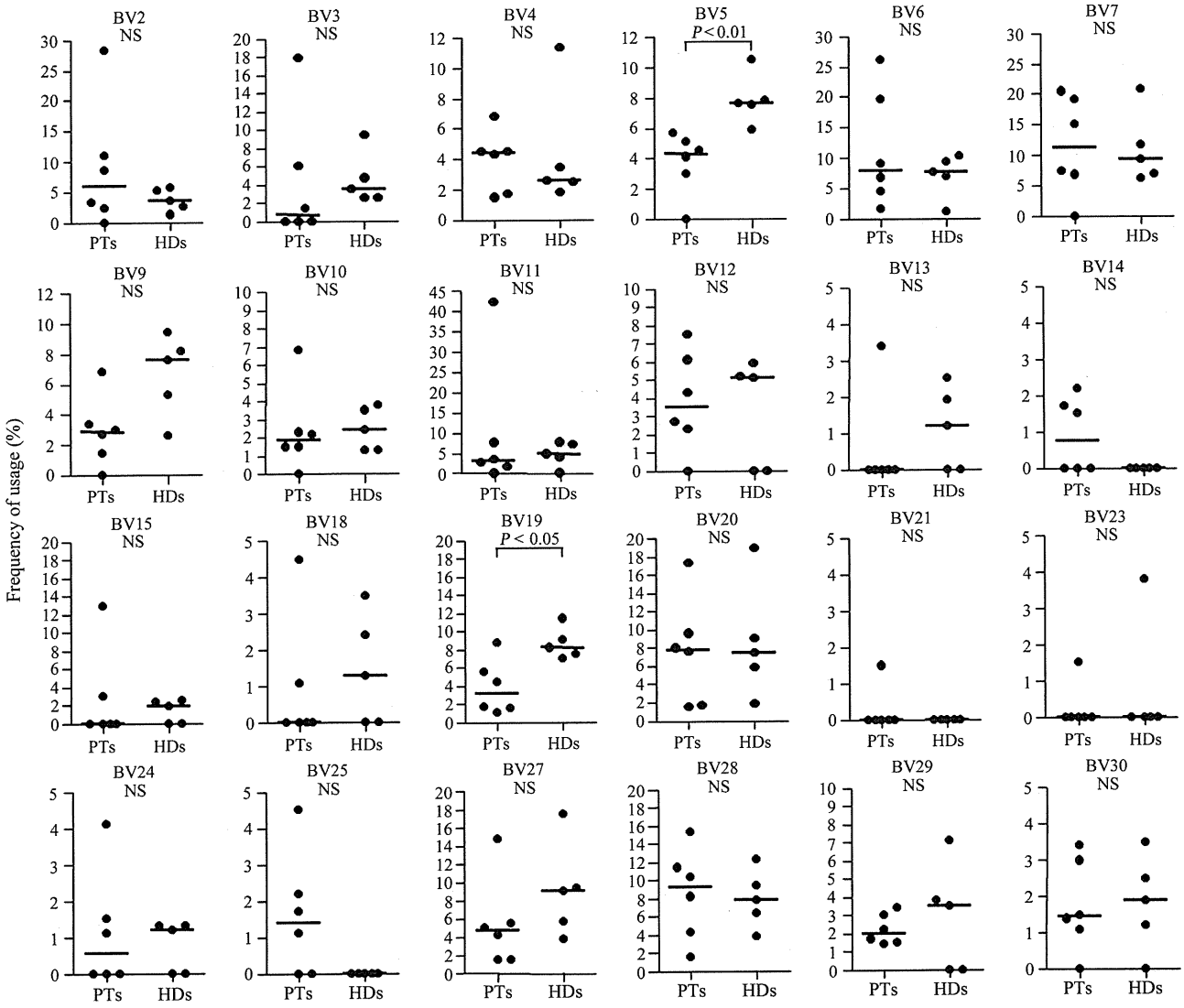

Fig. 4. Statistical comparison of usage frequencies of individual T cell receptor β-chain variable region (TCR-BV) gene families in $WT1_{126}$ tetramer$^+$ CD8$^+$ T cells between patients (PTs) and healthy donors (HDs). The significance of differences was assessed using the Mann–Whitney *U*-test. NS, not significant.

6, 7, 20, 27, and 28, while TCR-BV families 2, 11, and 15 were specifically biased in patients and TCR-BV families 4, 5, 9, and 19 were specifically biased in HDs. In total, six (3, 6, 7, 20, 27, and 28) of ten TCR-BV families (3, 4, 5, 6, 7, 9, 19, 20, 27, and 28) with biased usage in HDs also exhibited biased usage in patients. Three TCR-BV families (2, 11, and 15) newly emerged as those with biased usage specific to patients. However, in all BV gene families, except BVs 5 and 19, the usage frequencies did not differ significantly between patients and HDs. Together, these results led us to speculate that WT1-specific CTLs that had existed predominantly prior to the onset of the solid tumor had expanded and differentiated to maintain their dominance in tumor-bearing patients, whereas a few WT1-specific CTL populations with distinct TCR-BV families expanded in a tumor-bearing patient-specific manner. Furthermore, it may be suggested that WT1-specific CTLs with a dominant set of TCR-BV families in HDs play an important role in immune surveillance against tumors, and that the dominant populations continue to expand due to stimulation of the tumor-derived WT1 protein in WT1-expressing tumor-bearing patients. The immune response to WT1 may be unique, compared with other tumor-associated antigens, in the sense that WT1-specific CTLs are retained in healthy people at relatively higher levels, suggesting that precursors of WT1-specific CTLs are not deleted by the thymus, pass through it, and flow into the periphery. In fact, Pospori *et al.*[41] demonstrated that after murine hematopoietic stem cells transducted with the TCR gene of human HLA-A*0201-restricted WT1-specific CTLs had been transplanted into HLA-A*0201 transgenic recipients, surprisingly WT1-specific CTLs were not impaired by central or peripheral tolerance and, instead, differentiated into memory phenotype T cells. This suggests that precursors of WT1-specific CTLs are not deleted by the thymus. Thus, WT1-specific CTLs are likely to have some role in immune surveillance against tumors in both healthy people and patients with solid tumors. It appears reasonable that TCR-BV families that were appropriately selected for immune surveillance against tumors under healthy conditions were also preferentially used for immune surveillance under tumor conditions.

doi: 10.1111/j.1349-7006.2011.02163.x

The question as to whether different TCR-BV families are used in distinct differentiation subsets of $WT1_{126}$ tetramer$^+$ CD8$^+$ T cells was addressed in the present study. To resolve this issue, we analyzed differences in the usage frequencies of individual TCR-BV families between naïve and effector memory phenotypes, which are major and important phenotypes of $WT1_{126}$ tetramer$^+$ CD8$^+$ T cells. However, only PBMC from HD-3 and -4 were available for this experiment because they were relatively abundant, while those from the other HDs and patients were too few in number to be analyzed. The $WT1_{126}$ tetramer$^+$ CD8$^+$ T cells were divided into four cell populations of naïve, central memory, effector memory, and effector according to the cell surface expression of CCR7 and CD45RA, and both naïve and effector memory cell populations, which included more cells for the analysis, were provided for analysis of TCR-BV families. Eighteen naïve and nine effector memory cells from HD-3 and 26 naïve and 29 effector memory cells from HD-4 were FACS sorted and analyzed. As shown in Figure S1, available as Supplementary Material for this paper, usage frequencies of individual TCR-BV families were analyzed statistically between naïve and effector memory cell populations. In HD-3, no significant differences in usage frequencies of TCR-BV families were observed between naïve and effector memory cell populations. In addition, in HD-4, there were no significant differences in usage frequencies in most (13 of 15) of the TCR-BV families between the two cell populations, although the usage frequencies of only two TCR-BV families (i.e. BVs 12 and 19) were biased ($P = 0.0292$ and $P = 0.0019$, respectively). These results indicate that the usage pattern of TCR-BV families is similar between naïve- and effector memory-typed WT1-specific CTLs. These results also suggest that the patterns of biased usage of TCR-BV families does not change during the differentiation process from naïve to effector through central memory and effector memory.

In both patients and HDs, TCR-BV families 3, 6, 7, 20, 27 and 28 are preferentially used in $WT1_{126}$ tetramer$^+$ CD8$^+$ T cells. As for TCR-BV families of CTLs for other TAAs, it has been reported that, in a melanoma patient, HLA-A2-restricted NY-ESO-1-specific CD8$^+$ T cells preferentially used TCR-BV families 6, 9, and 12.[35] Among these three TCR-BV families, TCR-BV family 6 was also preferentially used by TCRs of $WT1_{126}$ tetramer$^+$ CD8$^+$ T cells in patients and HDs in the present study, while TCR-BV family 9 was preferentially used by $WT1_{126}$ tetramer$^+$ CD8$^+$ T cells in HDs. Thus, it is interesting to observe the phenomenon that a given set of TCR-BV families are preferentially used by certain TAA-specific CD8$^+$ T cells and that some of these families are shared by different TAA-specific CTLs. However, the reason why dominant CTLs for different TAAs (WT1 and NY-ESO-1) shared the same TCR-BV families 6 and 9 is difficult to explain at present. One explanation may be that TAA-specific CTLs with TCR-BV families 6 and 9 have an important role in tumor immunity in the context of HLA-A2 restriction. Further investigations are needed to address this issue.

Acknowledgments

This study was supported, in part, by a Grant-in-Aid from the Ministry of Education, Science, Sports, Culture, and Technology and the Ministry of Health, Labor, and Welfare of Japan.

Disclosure Statement

The authors have no conflicts of interest.

References

1 Drummond IA, Madden SL, Rohwer-Nutter P, Bell GI, Sukhatme VP, Rauscher FJ 3rd. Repression of the insulin-like growth factor II gene by the Wilms tumor suppressor WT1. *Science* 1992; **257**: 674–8.
2 Hewitt SM, Hamada S, McDonnell TJ, Rauscher FJ 3rd, Saunders GF. Regulation of the proto-oncogenes *bcl-2* and *c-myc* by the Wilms' tumor suppressor gene WT1. *Cancer Res* 1995; **55**: 5386–9.
3 Kim J, Prawitt D, Bardeesy N *et al.* The Wilms' tumor suppressor gene (*wt1*) product regulates *Dax-1* gene expression during gonadal differentiation. *Mol Cell Biol* 1999; **19**: 2289–99.
4 Call KM, Glaser T, Ito CY *et al.* Isolation and characterization of a zinc finger polypeptide gene at the human chromosome 11 Wilms' tumor locus. *Cell* 1990; **60**: 509–20.
5 Gessler M, Poustka A, Cavenee W, Neve RL, Orkin SH, Bruns GA. Homozygous deletion in Wilms tumours of a zinc-finger gene identified by chromosome jumping. *Nature* 1990; **343**: 774–8.
6 Yamagami T, Sugiyama H, Inoue K *et al.* Growth inhibition of human leukemic cells by WT1 (Wilms tumor gene) antisense oligodeoxynucleotides: implications for the involvement of WT1 in leukemogenesis. *Blood* 1996; **87**: 2878–84.
7 Inoue K, Tamaki H, Ogawa H *et al.* Wilms' tumor gene (WT1) competes with differentiation-inducing signal in hematopoietic progenitor cells. *Blood* 1998; **91**: 2969–76.
8 Tsuboi A, Oka Y, Ogawa H *et al.* Constitutive expression of the Wilms' tumor gene WT1 inhibits the differentiation of myeloid progenitor cells but promotes their proliferation in response to granulocyte-colony stimulating factor (G-CSF). *Leuk Res* 1999; **23**: 499–505.
9 Inoue K, Sugiyama H, Ogawa H *et al.* WT1 as a new prognostic factor and a new marker for the detection of minimal residual disease in acute leukemia. *Blood* 1994; **84**: 3071–9.
10 Bergmann L, Miething C, Maurer U *et al.* High levels of Wilms' tumor gene (wt1) mRNA in acute myeloid leukemias are associated with a worse long-term outcome. *Blood* 1997; **90**: 1217–25.
11 Tamaki H, Ogawa H, Ohyashiki K *et al.* The Wilms' tumor gene WT1 is a good marker for diagnosis of disease progression of myelodysplastic syndromes. *Leukemia* 1999; **13**: 393–9.
12 Oji Y, Ogawa H, Tamaki H *et al.* Expression of the Wilms' tumor gene WT1 in solid tumors and its involvement in tumor cell growth. *Jpn J Cancer Res* 1999; **90**: 194–204.
13 Oji Y, Suzuki T, Nakano Y *et al.* Overexpression of the Wilms' tumor gene WT1 in primary astrocytic tumors. *Cancer Sci* 2004; **95**: 822–7.
14 Oji Y, Yano M, Nakano Y *et al.* Overexpression of the Wilms' tumor gene WT1 in esophageal cancer. *Anticancer Res* 2004; **24**: 3103–8.
15 Cilloni D, Gottardi E, De Micheli D *et al.* Quantitative assessment of WT1 expression by real time quantitative PCR may be a useful tool for monitoring minimal residual disease in acute leukemia patients. *Leukemia* 2002; **16**: 2115–21.
16 Tamaki H, Mishima M, Kawakami M *et al.* Monitoring minimal residual disease in leukemia using real-time quantitative polymerase chain reaction for Wilms tumor gene (WT1). *Int J Hematol* 2003; **78**: 349–56.
17 Ogawa H, Tamaki H, Ikegame K *et al.* The usefulness of monitoring WT1 gene transcripts for the prediction and management of relapse following allogeneic stem cell transplantation in acute type leukemia. *Blood* 2003; **101**: 1698–704.
18 Oka Y, Elisseeva OA, Tsuboi A *et al.* Human cytotoxic T-lymphocyte responses specific for peptides of the wild-type Wilms' tumor gene (WT1) product. *Immunogenetics* 2000; **51**: 99–107.
19 Tsuboi A, Oka Y, Udaka K *et al.* Enhanced induction of human WT1-specific cytotoxic T lymphocytes with a 9-mer WT1 peptide modified at HLA-A*2402-binding residues. *Cancer Immunol Immunother* 2002; **51**: 614–20.
20 Oka Y, Udaka K, Tsuboi A *et al.* Cancer immunotherapy targeting Wilms' tumor gene WT1 product. *J Immunol* 2000; **164**: 1873–80.
21 Tsuboi A, Oka Y, Ogawa H *et al.* Cytotoxic T-lymphocyte responses elicited to Wilms' tumor gene WT1 product by DNA vaccination. *J Clin Immunol* 2000; **20**: 195–202.
22 Elisseeva OA, Oka Y, Tsuboi A *et al.* Humoral immune responses against Wilms tumor gene WT1 product in patients with hematopoietic malignancies. *Blood* 2002; **99**: 3272–9.
23 Wu F, Oka Y, Tsuboi A *et al.* Th1-biased humoral immune responses against Wilms tumor gene WT1 product in the patients with hematopoietic malignancies. *Leukemia* 2005; **19**: 268–74.
24 Gaiger A, Carter L, Greinix H *et al.* WT1-specific serum antibodies in patients with leukemia. *Clin Cancer Res* 2001; **7**: 761s–5s.

25 Cheever MA, Allison JP, Ferris AS *et al.* The prioritization of cancer antigens: a national cancer institute pilot project for the acceleration of translational research. *Clin Cancer Res* 2009; **15**: 5323–37.
26 Oka Y, Tsuboi A, Taguchi T *et al.* Induction of WT1 (Wilms' tumor gene)-specific cytotoxic T lymphocytes by WT1 peptide vaccine and the resultant cancer regression. *Proc Natl Acad Sci U S A* 2004; **101**: 13885–90.
27 Kawakami M, Oka Y, Tsuboi A *et al.* Clinical and immunologic responses to very low-dose vaccination with WT1 peptide (5 microg/body) in a patient with chronic myelomonocytic leukemia. *Int J Hematol* 2007; **85**: 426–9.
28 Kaida M, Morita-Hoshi Y, Soeda A *et al.* Phase 1 trial of Wilms tumor 1 (WT1) peptide vaccine and gemcitabine combination therapy in patients with advanced pancreatic or biliary tract cancer. *J Immunother* 2011; **34**: 92–9.
29 Rezvani K, Yong AS, Mielke S *et al.* Repeated PR1 and WT1 peptide vaccination in montanide-adjuvant fails to induce sustained high-avidity, epitope-specific CD8+ T cells in myeloid malignancies. *Haematologica* 2011; **96**: 432–40.
30 Tanaka-Harada Y, Kawakami M, Oka Y *et al.* Biased usage of BV gene families of T-cell receptors of WT1 (Wilms' tumor gene)-specific CD8+ T cells in patients with myeloid malignancies. *Cancer Sci* 2010; **101**: 594–600.
31 Nakatsuka S, Oji Y, Horiuchi T *et al.* Immunohistochemical detection of WT1 protein in a variety of cancer cells. *Mod Pathol* 2006; **19**: 804–14.
32 Valmori D, Scheibenbogen C, Dutoit V *et al.* Circulating tumor-reactive CD8(+) T cells in melanoma patients contain a CD45RA(+)CCR7(−) effector subset exerting *ex vivo* tumor-specific cytolytic activity. *Cancer Res* 2002; **62**: 1743–50.
33 Sallusto F, Lenig D, Förster R, Lipp M, Lanzavecchia A. Two subsets of memory T lymphocytes with distinct homing potentials and effector functions. *Nature* 1999; **401**: 708–12.
34 Valmori D, Dutoit V, Liénard D *et al.* Tetramer-guided analysis of TCR beta-chain usage reveals a large repertoire of melan-A-specific CD8+ T cells in melanoma patients. *J Immunol* 2000; **165**: 533–8.
35 Derré L, Bruyninx M, Baumgaertner P *et al.* *In vivo* persistence of codominant human CD8+ T cell clonotypes is not limited by replicative senescence or functional alteration. *J Immunol* 2007; **179**: 2368–79.
36 Wadia P, Rao D, Pradhan T, Pathak A, Chiplunkar S. Impaired lymphocyte responses and their restoration in oral cancer patients expressing distinct TCR variable region. *Cancer Invest* 2008; **26**: 471–80.
37 Dietrich PY, Walker PR, Quiquerez AL *et al.* Melanoma patients respond to a cytotoxic T lymphocyte-defined self-peptide with diverse and nonoverlapping T-cell receptor repertoires. *Cancer Res* 2001; **61**: 2047–54.
38 Willhauck M, Möhler T, Scheibenbogen C *et al.* T-cell receptor beta variable region diversity in melanoma metastases after interleukin 2-based immunotherapy. *Clin Cancer Res* 1996; **2**: 767–72.
39 Mandruzzato S, Rossi E, Bernardi F *et al.* Large and dissimilar repertoire of Melan-A/MART-1-specific CTL in metastatic lesions and blood of a melanoma patient. *J Immunol* 2002; **169**: 4017–24.
40 Zhou J, Dudley ME, Rosenberg SA, Robbins PF. Selective growth, *in vitro* and *in vivo*, of individual T cell clones from tumor-infiltrating lymphocytes obtained from patients with melanoma. *J Immunol* 2004; **173**: 7622–9.
41 Pospori C, Xue SA, Holler A *et al.* Specificity for the tumor-associated self-antigen WT1 drives the development of fully functional memory T cells in the absence of vaccination. *Blood* 2011; **117**: 6813–24.

Supporting Information

Additional Supporting Information may be found in the online version of this article:

Fig. S1. Statistical comparison of usage frequencies of T cell receptor β-chain variable region (TCR-BV) gene families in $WT1_{126}$ tetramer$^+$ $CD8^+$ T cells between naïve and effector memory fractions.

Please note: Wiley-Blackwell are not responsible for the content or functionality of any supporting materials supplied by the authors. Any queries (other than missing material) should be directed to the corresponding author for the article.

doi: 10.1111/j.1349-7006.2011.02163.x

Vaccine 30 (2012) 722–729

Contents lists available at SciVerse ScienceDirect

Vaccine

journal homepage: www.elsevier.com/locate/vaccine

Enhanced tumor immunity of WT1 peptide vaccination by interferon-β administration☆

Hiroko Nakajima[a], Yoshihiro Oka[b], Akihiro Tsuboi[c], Naoya Tatsumi[d], Yumiko Yamamoto[e], Fumihiro Fujiki[a], Zheyu Li[e], Ayako Murao[b], Soyoko Morimoto[b], Naoki Hosen[e], Toshiaki Shirakata[e,f], Sumiyuki Nishida[c], Ichiro Kawase[b], Yoshitaka Isaka[g], Yusuke Oji[d], Haruo Sugiyama[e,*]

[a] Department of Cancer Immunology, Osaka University Graduate School of Medicine, Osaka, Japan
[b] Department of Respiratory Medicine, Allergy and Rheumatic Diseases, Osaka University Graduate School of Medicine, Osaka, Japan
[c] Department of Cancer Immunotherapy, Osaka University Graduate School of Medicine, Osaka, Japan
[d] Department of Cancer Stem Cell Biology, Osaka University Graduate School of Medicine, Osaka, Japan
[e] Department of Functional Diagnostic Science, Osaka University Graduate School of Medicine, 1-7, Yamada-Oka, Suita City, Osaka 565-0871, Japan
[f] Department of Bioregulatory Medicine, Ehime University Graduate School of Medicine, Toon, Ehime, Japan
[g] Department of Nephrology, Osaka University Graduate School of Medicine, Osaka, Japan

ARTICLE INFO

Article history:
Received 18 August 2011
Received in revised form
18 November 2011
Accepted 19 November 2011
Available online 29 November 2011

Key words:
WT1
IFN-β
Immunotherapy
Cancer vaccine
Adjuvant

ABSTRACT

To induce and activate tumor-associated antigen-specific cytotoxic T lymphocytes (CTLs) for cancer immunity, it is important not only to select potent CTL epitopes but also to combine them with appropriate immunopotentiating agents. Here we investigated whether tumor immunity induced by WT1 peptide vaccination could be enhanced by IFN-β. For the experimental group, C57BL/6 mice were twice pre-treated with WT1 peptide vaccine, implanted with *WT1*-expressing C1498 cells, and treated four times with WT1 peptide vaccine at one-week intervals. During the vaccination period, IFN-β was injected three times a week. Mice in control groups were treated with WT1 peptide alone, IFN-β alone, or PBS alone. The mice in the experimental group rejected tumor cells and survived significantly longer than mice in the control groups. The overall survival on day 75 was 40% for the mice treated with WT1 peptide + IFN-β, while it was 7, 7, and 0% for those treated with WT1 peptide alone, IFN-β alone or PBS alone, respectively. Induction of WT1-specific CTLs and enhancement of NK activity were detected in splenocytes from mice in the experimental group. Furthermore, administration of IFN-β enhanced expression of MHC class I molecules on the implanted tumor cells. In conclusion, our results showed that co-administration of WT1 peptide + IFN-β enhanced tumor immunity mainly through the induction of WT1-specific CTLs, enhancement of NK activity, and promotion of MHC class I expression on the tumor cells. WT1 peptide vaccination combined with IFN-β administration can thus be expected to enhance the clinical efficacy of WT1 immunotherapy.

1. Introduction

Induction and activation of tumor-associated antigen (TAA)-specific cytotoxic T lymphocytes (CTLs) is essential for cancer immunotherapy. For this purpose, it is important to co-administer appropriate immunopotentiating agents, including adjuvants or cytokines, together with a TAA-derived peptide that serves as a CTL epitope, because injection of a CTL epitope alone cannot sufficiently induce and activate the TAA-specific CTLs. Furthermore, if the co-administered agents not only help induction/activation of the CTLs but also activate other effector cells such as NK cells, this may further enhance anti-tumor responses.

The Wilms' tumor gene *WT1* was originally isolated as a gene responsible for Wilms' tumor, a pediatric renal cancer [1,2]. This gene encodes a zinc finger transcription factor involved in organ development, cell proliferation and differentiation, as well as apoptosis. The *WT1* gene product regulates the expression of various genes either positively or negatively, depending upon how it combines with other regulatory proteins in different types of cells. Although *WT1* was categorized at first as a tumor suppressor gene [3], we have proposed that the wild-type *WT1* gene plays an oncogenic rather than a tumor-suppressor gene function in leukemogenesis/tumorigenesis on the basis of the following

☆ This study was supported in part by a Grant-in-Aid from the Ministry of Education, Culture, Sports, Science and Technology and the Ministry of Health, Labor, and Welfare, Japan.

* Corresponding author. Tel.: +81 6 6879 2593; fax: +81 6 6879 2593.
E-mail address: sugiyama@sahs.med.osaka-u.ac.jp (H. Sugiyama).

0264-410X/$ – see front matter © 2011 Elsevier Ltd. All rights reserved.
doi:10.1016/j.vaccine.2011.11.074

findings: (i) the wild-type *WT1* gene was highly expressed in leukemias and solid cancers [4–17]; (ii) high expression levels of *WT1* mRNA correlated with poor prognosis in leukemia and several kinds of solid cancer [4]; (iii) growth of *WT1*-expressing leukemia and solid cancer cells was inhibited by treatment with *WT1* antisense oligomers *in vitro* [18]; and (iv) in wild-type *WT1* gene-transfected myeloid progenitor cells, differentiation was blocked but proliferation was induced in response to granulocyte colony-stimulating factor [19,20]. These findings indicate that *WT1* over-expression and leukemogenesis/tumorigenesis may be closely related, which suggests that the wild-type *WT1* gene product could be a promising tumor rejection antigen for cancer immunotherapy. In fact, we [14–17,21] and others [22,23] have generated human WT1-specific CTLs *in vitro*, and we were able to show that mice immunized with MHC class I-restricted WT1 peptide or with *WT1* plasmid DNA elicited WT1-specific CTLs and rejected the challenge of *WT1*-expressing cancer cells *in vivo* [14–17,24,25], while the induced CTLs did not damage normal tissue cells that physiologically expressed *WT1*, including kidney podocytes and bone marrow (BM) stem/progenitor cells. Furthermore, we demonstrated that WT1 peptide vaccination combined with *Mycobacterium bovis* bacillus Calmette-Guérin cell wall skeleton (BCG-CWS) [26], which was injected one day previously at the same site as the WT1 peptide was more effective for eradication of *WT1*-expressing tumors than treatment with WT1 peptide alone or BCG-CWS alone [27]. BCG-CWS strongly activated dendritic cells (DCs) of the injection sites, i.e. activated of innate immunity, and also induced/activated of TAA (WT1)-specific CTLs.

Interferon-β (IFN-β) is a Type I interferon, and is known for its various immunopotentiating properties: (i) enhancement of the expression of many surface molecules that are essential for binding and/or activation of CTLs, in particular the major histocompatibility complex (MHC) class I as well as the receptors B7-1 (CD80) and intercellular adhesion molecule-1 (ICAM-1) [28,29], on antigen-presenting cells (APCs) or cancer cells; (ii) activation of NK, B, and T cells [30,31]; (iii) a direct anti-proliferation effect on cancer cells by promoting cell cycle arrest at the G1 phase [32]; (iv) induction of apoptosis of cancer cells [33]; and (v) inhibition of angiogenesis [34]. In fact, it was reported in mouse models that type I interferon was essential in the induction of CTL and eradication of EG-7 tumors expressing ovalbumin in mice by vaccination with CpG-adjuvanted ovalbumin [35], and that type I interferon augmented induction of CTL through DNA-based vaccination [36]. Furthermore, IFN-β has already been in use for cancer immunotherapy in clinical settings [37–40], and the mechanism for the enhancement of immunity against cancer has been thoroughly investigated. The results show that IFN-β should be considered as one of the most promising immunopotentiating agents for use with TAA-directed cancer vaccines.

We examined whether WT1 peptide vaccination combined with IFN-β administration leads to greater enhancement of tumor cell rejection than WT1 peptide vaccination alone in a mouse model and we tried to elucidate the mechanisms of enhancement of WT1 immunity by the co-administration of IFN-β.

2. Materials and methods

2.1. Mice

Male C57BL/6 (H-2D^b) mice were purchased from Clea Japan, Inc. (Tokyo, Japan), maintained in a specific pathogen-free (SPF) containment facility in accordance with the guidelines of Osaka University, and used for experiments at 6–8 weeks of age.

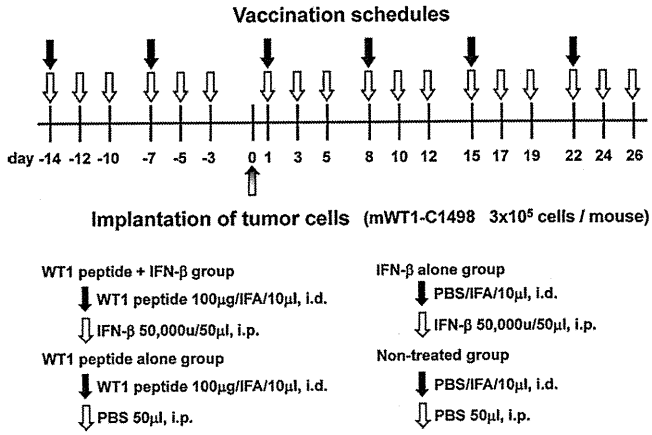

Fig. 1. *In vivo* tumor cell challenge and vaccination schedule. Mice were intradermally (i.d.) and abdominally pre-immunized with 100 μg WT1 peptide emulsified in incomplete Freund's adjuvant (IFA, Montanide ISA51) on day −14 and −7. Concomitantly, 50,000 units of murine IFN-β was intraperitoneally (i.p.) injected three times per week during the two weeks before tumor cell implantation. On day 0, mice were subcutaneously implanted with 3×10^5 mWT1-C1498 cells in 100 μl of PBS. This was followed by abdominal injection of 100 μg WT1 peptide emulsified in IFA on days 1, 8, 15 and 22. In addition 50,000 units of murine IFN-β was also i.p. injected three times per week until day 26 (WT1 peptide + IFN-β group). Mice in the control groups were injected with WT1 peptide emulsified in IFA and PBS (WT1 peptide alone group), PBS emulsified in IFA and IFN-β (IFN-β alone group), or PBS emulsified in IFA and PBS (non-treated group).

2.2. Reagents

An MHC class I (H-2D^b)-binding peptide, Db126 peptide (a.a.126-134 RMFPNAPYL), was synthesized by SIGMA Genosys (Ishikari, Japan) [24]. The peptide was dissolved in PBS and stored at −20 °C until use. Murine IFN-β was kindly donated by Toray Industries (Tokyo, Japan). Montanide ISA 51, an incomplete Freund's adjuvant (IFA), was purchased from Seppic S.A. (Orsay, France). Anti-CD8 and anti-NK1.1 mAbs for cell depletion were produced by 53-6.7.2 and PK136 hybridoma clones, respectively. Both hybridoma were obtained from American Type Culture Collection (ATCC, Rockville, MD, USA).

2.3. Cells

C1498, a *WT1*-nonexpressing murine leukemia cell line of C57BL/6 origin, was obtained from ATCC (Rockville, MD, USA). *WT1*-expressing murine WT1-C1498 (mWT1-C1498) was generated by transduction of C1498 cells with CMV promoter driven murine WT1 17AA(+)KTS(+) isoform full length cDNA that was inserted into pcDNA3.1(+) mammalian expression vector (Invitrogen, Tokyo, Japan). YAC-1 cells that were used as target cells for NK activity were obtained from ATCC. RMAS, a TAP-deficient subline of RMA (Rauscher leukemia virus-induced lymphoma cell line of C57BL/6 origin), was kindly provided by Dr. K. Kärre (Karolinska Institute, Sweden) through Dr. H.-G. Rammensee (University of Tübingen, Germany) [24].

2.4. In vivo tumor cell challenge and vaccination schedule

The implanted dose of the tumor cells was optimized by preliminary experiments in which more than 90% of the non-treated mice transplanted with the tumor cells died within two months due to tumor development. We therefore adopted an observation period of 75 days after the tumor cell implantation (day 0). Tumor implantation and vaccination schedule are shown in Fig. 1. Mice were intradermally (i.d.) pre-immunized with an abdominal injection of 100 μg WT1 peptide emulsified with IFA on days −14 and

–7. During the same period, 50,000 units of murine IFN-β was intraperitoneally (i.p.) injected three times per week. On day 0, mice were subcutaneously (s.c.) implanted with 3×10^5 mWT1-C1498 cells in 100 μl of PBS, followed by abdominal i.d. injection of 100 μg WT1 peptide emulsified with IFA on days 1, 8, 15, and 22. In addition, 50,000 units of murine IFN-β was also injected i.p. three times per week until day 26. Mice in control groups were vaccinated with WT1 peptide + IFA + PBS (WT1 peptide alone group); PBS + IFA + IFN-β (IFN-β alone group); and PBS + IFA + PBS (non-treated group). Tumor growth was monitored by measuring the longest diameter of the palpable mass.

For the assessment of immunological effector cells, we performed *in vivo* experiments independently from those for the assessment of survival. Splenocytes and bone marrow cells from mice immunized as shown in Fig. 1 were recovered on day 30 (8 days after the last vaccination) and used for ^{51}Cr release cytotoxicity assay (CTL and NK activities) and colony assay, respectively. Furthermore, the resected tumors were used for analysis of MHC class I expression.

2.5. ^{51}Cr release cytotoxicity assay and mice treatment schedule for the assay

Splenocytes were stimulated with the 5 μg/ml WT1 peptide and cultured in complete medium containing 10% heat-inactivated FCS, 45% RPMI1640 medium, 45% AIM-V medium, 1× non-essential amino acid (Gibco), 25 ng/ml 2-mercaptoethanol, 50 IU/ml penicillin and 50 μg/ml streptomycin. Two and four days later, recombinant interleukin-2 (rIL-2; kindly donated by Shionogi Biomedical Laboratories, Osaka, Japan) was added to the culture at a concentration of 20 IU/ml. After six days of culture, a ^{51}Cr release cytotoxicity assay was performed against WT1 peptide-pulsed or -unpulsed RMAS cells for WT1-specific CTL activity, and against YAC-1 cells for NK cell activity, as described previously [24]. Target cells (1×10^4 cells) labeled with ^{51}Cr were added to wells containing varying numbers of effector cells in 96-well plates. After 4 h of incubation at 37 °C, cell lysates were centrifuged and 100 μl of the supernatant was collected and measured for radioactivity. The percentage of specific lysis (% specific lysis) was calculated as follows: percentage of specific lysis = (cpm of experimental release – cpm of spontaneous release)/(cpm of maximal release – cpm of spontaneous release) × 100. Radioactivity of the supernatant, either of the target cell cultures without effector cells, or of the target cells that were completely lysed by the treatment with 1% Triton X-100 was used for spontaneous and maximal release, respectively.

2.6. Analysis of MHC class I expression

Tumors were resected from the tumor-bearing mice on day 30, and tumor cell suspensions were prepared with the tissues in the center of the tumor mass. The resected tissues contained only tumor mass with the naked eye. The cells were stained with FITC-conjugated anti-mouse H-2D^b monoclonal antibody (KH-95, BD Biosciences, Franklin Lakes, NJ, USA) and analyzed with the FACSort (BD). Live cells were determined by means of FSC and SSC gating.

2.7. Colony assay

For CFU-GM (colony-forming-unit granulocyte-macrophage) assay, bone marrow cells were recovered from mice on day 30, plated at 1×10^4 cells/plate in methylcellulose medium containing 10 ng/ml IL-3, 10 ng/ml IL-6, 50 ng/ml SCF, and 3 U/ml erythropoietin (EPO) (Methocult M3434; Stem Cell Technologies, Vancouver, BC, Canada), and cultured at 37 °C in a humidified incubator under 5% CO_2. Colonies with more than 50 cells were counted on days 8 and 12.

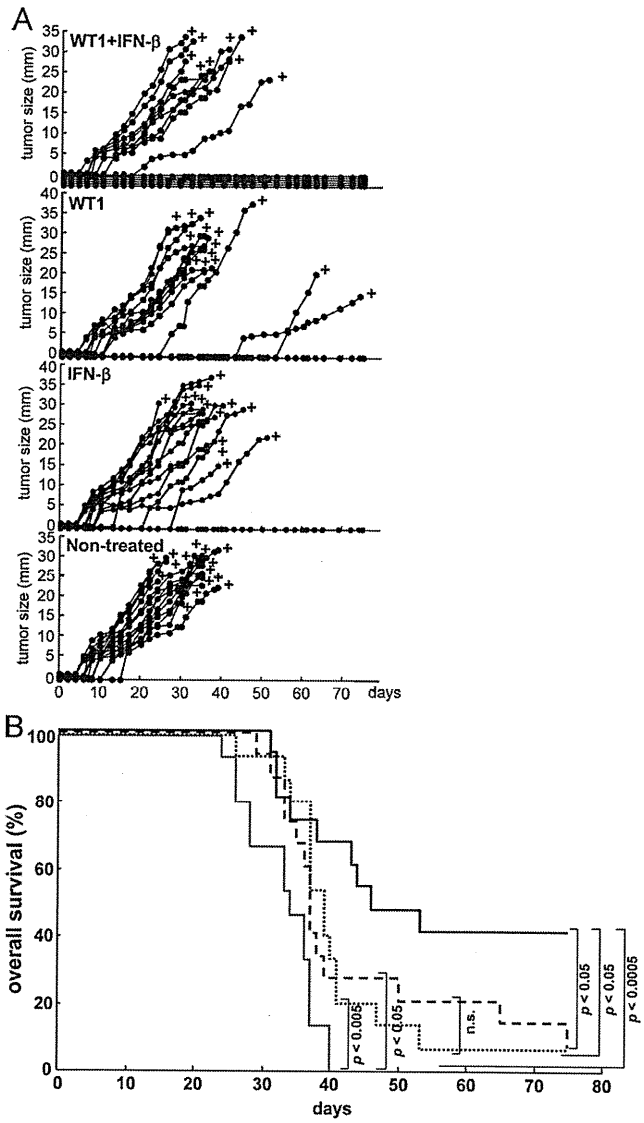

Fig. 2. Effect of WT1 peptide vaccination combined with IFN-β administration on rejection of implanted tumor cells. (A) Time course of size of tumors developed in individual mice of the four groups. Tumor sizes represent the longest diameters. (B) Overall survival curves of the four groups. Solid black, broken, dotted, and solid gray lines represent overall survival curves of mice treated with WT1 peptide vaccine + IFN-β, WT1 peptide vaccine alone, IFN-β alone, and non-treated mice, respectively.

2.8. In vivo CD8$^+$ T and NK cell depletion experiments

Mice were implanted with 3×10^5 mWT1-C1498 cells and treated with WT1 peptide vaccine + IFN-β as shown Fig. 1. The WT1- and IFN-β- treated mice were injected with PBS or 200 μg of anti-CD8 and/or 200 μg of anti-NK mAbs on days –15, –8, –1, 4, 7, 11, 14, 18, 21 and 25 [35,41].

2.9. Statistical analysis

Significant differences in overall survivals among experimental groups were evaluated with the Logrank test. The Student's *t*-test was used to calculate the differences in the expression levels of H-2D^b on tumor cells in mice among experimental groups.

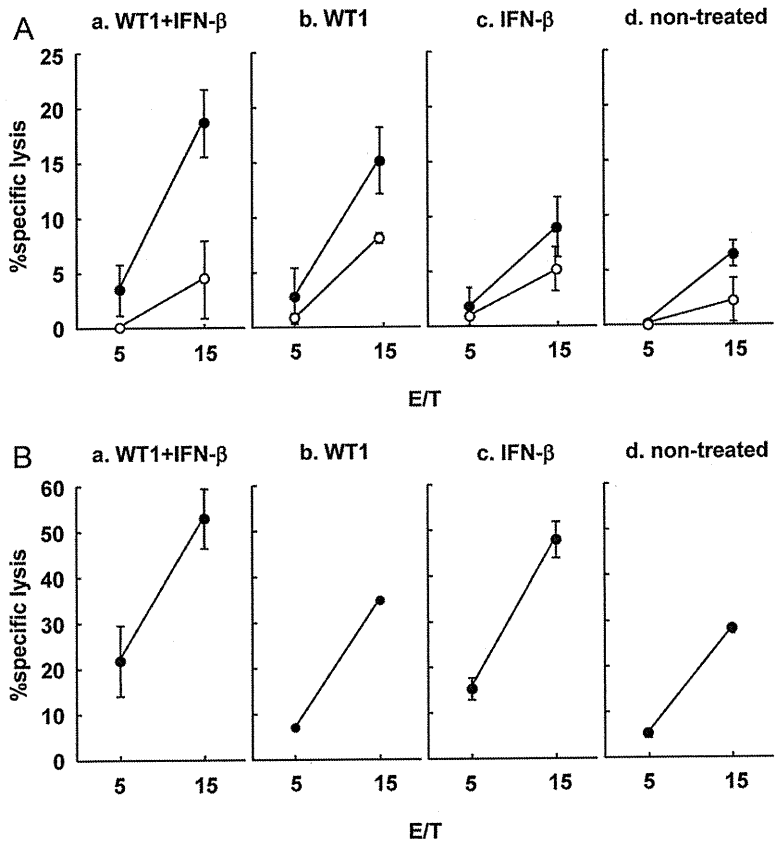

Fig. 3. Induction of WT1-specifc CTLs and enhancement of NK activity by treatment with WT1 peptide vaccine + IFN-β. Eight days after the last vaccination, splenocytes from the mice in each group were stimulated *in vitro* with WT1 peptide-pulsed synergistic splenocytes. WT1-specific CTL and NK cell activities were assayed in triplicate as cytotoxic activities against WT1 peptide-pulsed, -unpulsed RMAS or YAC-1 cells, respectively, at the indicated E/T ratio. (A) WT1-specific CTL activity. Closed and open circles represent cytotoxic activities against WT1 peptide-pulsed or -unpulsed RMAS, respectively. (B) NK activity. NK activity is shown as cytotoxic activities against YAC-1 cells. Bars indicate standard errors.

3. Results

3.1. IFN-β promotes efficacy of WT1 peptide vaccination

To investigate whether IFN-β promoted tumor cell rejection by WT1 peptide vaccination, mice were twice immunized with Montanide ISA51-emulsified WT1 peptide with or without IFN-β administration before transplantation of *WT1*-expressing tumor cells (mWT1-C1498) and then repeatedly WT1-immunized, followed by assessment of the tumor growth and their survival (Fig. 1). Optimization of cell number and determination of the observation period are described in Section 2.

Nine of the 15 mice treated with WT1 peptide vaccine + IFN-β developed tumors and died, while the remaining 6 mice were alive without tumors on day 75 (Fig. 2A). In contrast, 14 of the 15 mice treated with WT1 peptide vaccine alone, 14 of the 15 mice treated with IFN-β alone and all of the 15 non-treated mice had died of tumor growth by day 75. Overall survival rates on day 75 were 40% for mice treated with WT1 peptide vaccine + IFN-β, but 7, 7 and 0% for mice treated with WT1 peptide vaccine alone or IFN-β alone or for non-treated mice, respectively. The overall survival rates of mice treated with WT1 peptide vaccine + IFN-β were significantly higher than those of the other three groups (WT1 peptide vaccine + IFN-β versus WT1 peptide vaccine alone, IFN-β alone or non-treated: $p < 0.05$, $p < 0.05$, and $p < 0.0005$, respectively). The overall survival rates of mice treated with WT1 peptide vaccine alone or IFN-β alone were significantly higher than those of non-treated (WT1 peptide vaccine alone versus non-treated, IFN-β alone versus non-treated: $p < 0.05$ and $p < 0.005$, respectively). There was no significant difference in survival rate between WT1 peptide vaccine alone and IFN-β alone (Fig. 2B).

3.2. WT1 peptide vaccine + IFN-β enhances induction of WT1-specific CTLs and activates NK cell activity

In order to analyze immune responses, tumor-bearing mice treated with WT1 peptide vaccine + IFN-β as shown in Fig. 1 were sacrificed on day 30. The splenocytes of each mouse were stimulated *in vitro* with WT1 peptide and assayed for WT1 peptide-specific CTL activity against WT1 peptide-pulsed and -unpulsed RMAS cells and for NK activity against YAC-1 cells. Representative data are shown in Fig. 3. Splenocytes from mice treated with WT1 peptide vaccine + IFN-β showed the strongest WT1 peptide-specific cytotoxic activity while splenocytes from non-treated mice showed the weakest activity. WT1-specific cytotoxic activity was in the following order: WT1 peptide vaccine + IFN-β > WT1 peptide vaccine alone > IFN-β alone > non-treated. These findings convincingly showed that WT1-specific CTL activity was higher in the two groups with WT1 peptide vaccine than in the two groups without it. It appeared that the WT1-specific CTL activities in splenocytes from IFN-β-treated or non-treated mice were endogenously induced as a result of immunological stimulation by *WT1*-expressing tumor cells implanted.

Next, NK cell activity was examined (Fig. 3B). Mice of all four groups were sacrificed on day 30 and their splenocytes were analyzed for their NK cell activity. NK cell activity was higher in both

WT1 peptide vaccine + IFN-β and IFN-β alone groups. These results suggested that NK activity was endogenously induced in *WT1*-expressing tumor-bearing mice and that this activity was enhanced by administration of IFN-β, which is a potent enhancer of NK activity.

Taken together, these results indicated that the strongest rejection of implanted tumor cells in the mice treated with WT1 peptide vaccine + IFN-β resulted from the generation of the highest levels of both WT1-specific CTLs and NK cells.

3.3. *WT1 specific CTLs and NK cells play crucial roles in the treatment by WT1 peptide vaccine + IFN-β*

To confirm that WT1-specific CTLs and NK cells played crucial roles in the tumor rejection, *in vivo* depletion of $CD8^+$ T and/or NK cells was performed. Mice that were implanted with mWT1-C1498 cells and vaccinated with WT1 peptide vaccine + IFN-β as shown in Fig. 1 were treated with both or either of anti-CD8 and anti-NK mAbs.

Tow of five mAb-non-treated mice developed tumors and died, while the remaining three survived without development of tumors. In contrast, all of the mice that were treated with both or either of anti-CD8 and anti-NK mAbs and vaccination-non-treated mice died of tumor development. It should be noted that appearance of tumors in mice treated with both or either anti-CD8 and anti-NK mAbs was earlier than that in mAb-non-treated mice (Fig. 4).

These results strongly indicated that both WT1-specific $CD8^+$ CTLs and NK cells played crucial roles in the rejection of tumor cells.

3.4. *Enhancement of MHC class I (H-2D^b) expression on transplanted tumor cells by the administration of IFN-β*

Since WT1 (Db126) peptide is produced from WT1 protein through processing in tumor cells and presents on the cell surface in association with MHC class I (H-2D^b) [29,32], H-2D^b expression levels of target cells are thought to exert a major influence on the susceptibility of the cells to attack by vaccination-induced WT1 (Db126)-specific CTLs. For this reason, the H-2D^b expression levels on the transplanted tumor cells (*WT1*-expressing C1498 cells) were examined. Tumor-bearing mice were sacrificed 30 days after tumor cell implantation, the tumors were resected, and the tumor cells were stained with anti-H-2D^b antibody (Fig. 5). The expression levels of H-2D^b on tumor cells was significantly higher in mice treated with WT1 peptide vaccine + IFN-β or IFN-β alone than in those treated with WT1 peptide vaccine alone or non-treated mice ($p < 0.05$) (Fig. 5B). These results indicated that IFN-β administration enhanced the expression of H-2D^b on tumor cells, which should make tumor cells more susceptible to attack by WT1-specific CTLs.

3.5. *No inhibition of colony-forming ability of bone marrow cells from mice immunized with WT1 peptide vaccine + IFN-β*

WT1 is expressed in some tissues of normal adult mice, including hematopoietic stem/progenitor cells, podocytes of kidney glomeruli, gonads and mesothelial structures. To evaluate the risk of induction of autoimmunity by immunization with WT1 peptide vaccine + IFN-β, the colony-forming ability of bone marrow cells, as shown by the numbers of CFU-GM colonies, were examined. No differences in numbers of CFU-GM colonies were found among the five groups (WT1 peptide vaccine + IFN-β, WT1 peptide vaccine alone, IFN-β alone, tumor-bearing non-treated, and non-tumor-bearing non-treated) (Fig. 6). These results showed that induced

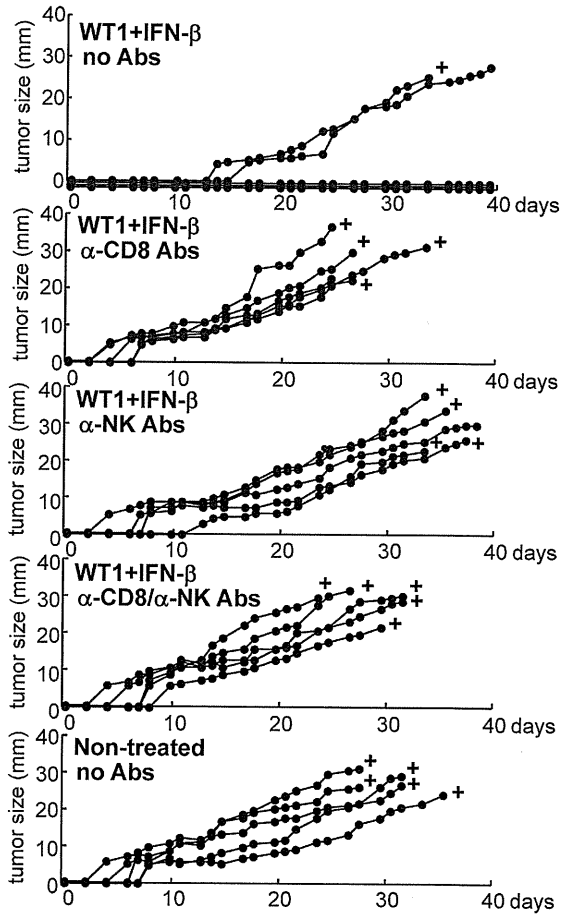

Fig. 4. Cancellation of tumor rejection by WT1 peptide vaccine + IFN-β by the administration of anti-CD8 and/or anti-NK mAbs. Mice were implanted with 3×10^5 mWT1-C1498 cells and treated with WT1 peptide vaccine + IFN-β as shown in Fig. 1. The WT1- and IFN-β- treated mice were injected with PBS or 200 μg of anti-CD8 and/or 200 μg of anti-NK mAbs on days −15, −8, −1, 4, 7, 11, 14, 18, 21 and 25. Time course of size of tumors developed in individual mice from the five groups. Tumor sizes represent the longest diameters.

WT1-specific CTLs did not recognize normal cells that physiologically expressed *WT1*.

4. Discussion

In the study presented here, we demonstrated that co-treatment with WT1 peptide vaccine (Db126; CTL epipope) + IFN-β enhanced rejection of *WT1*-expressing tumor cells in a mouse model. Enhanced induction of WT1-specific CTLs and NK cell activity was considered to be largely responsible for the successful rejection of the implanted tumor cells. The important roles of WT1-specific $CD8^+$ T cells and NK cells in the tumor rejection were confirmed by depletion experiments using anti-CD8 and/or anti-NK mAbs.

The most likely mechanism for the induction of the strongest WT1-specific cytotoxic activity in mice treated with WT1 peptide vaccine + IFN-β is the following: IFN-β activates NK cells [30,42,45], which generate IFN-γ, which in turn activates DCs and T cells [42–44]. Furthermore, IFN-β can also activate T cells directly [30]. These conditions lead to a more efficient induction of WT1-specific CTLs by the WT1 peptide vaccine. The WT1 peptide-specific cytotoxic activity observed in tumor-bearing non-treated mice may be due to the spontaneous induction of WT1-specific CTLs as a result of immune stimulation by implanted *WT1*-expressing tumors. Enhancement of NK cell function induced by *in vivo*

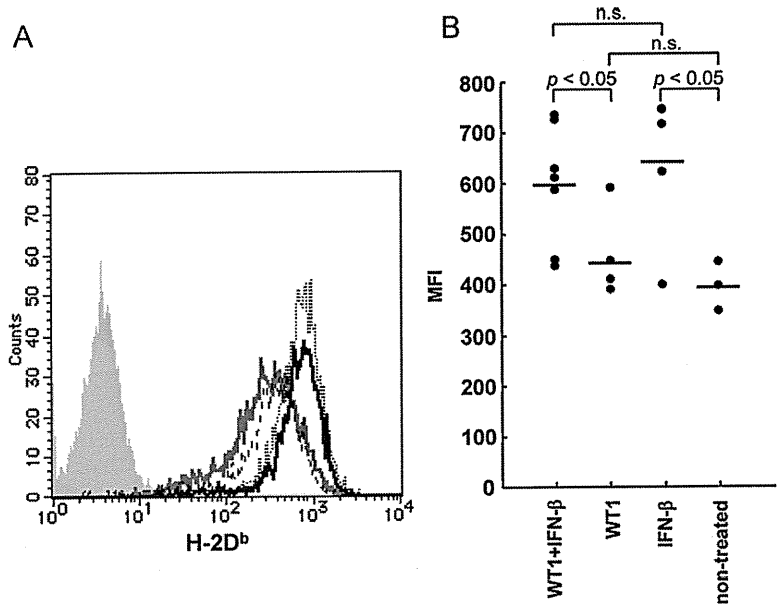

Fig. 5. IFN-β enhanced MHC class I (H-2D^b) expression of tumor cells *in vivo*. (A) H-2D^b expression levels of tumor cells recovered from mice. Solid black, broken, dotted, and solid gray lines represent the expression levels of tumor cells from mice treated with WT1 peptide vaccine + IFN-β, WT1 peptide vaccine alone, or IFN-β alone, and non-treated mice, respectively. (B) The mean fluorescence intensity (MFI) of H-2D^b expression of tumor cells from mice.

administration of IFN-β contributed to a high rejection rate of tumors in the present experiment system. However, the exact mechanism of the enhancement was not addressed in this study, while a series of investigations regarding the effect of IFN-β on NK cells were reported, including that IFN-β upregulated TRAIL on NK cells [45] and enhanced production of IFN-γ from NK cells. Besides NK cells, NKT cells might also have important roles in enhancement of tumor rejection in the present experiment system, considering that it was reported that IFN-β enhanced up-regulation of CD1d on DCs, which leads to NKT cell activation [46]. Further studies are needed to address the mechanism of enhancement of NK and NKT cell function by IFN-β in the context of tumor immunity.

At least two merits of IFN-β administration could be confirmed. One was that, as shown in Fig. 3B, greater enhancement of NK cell activity was observed in mice treated with WT1 peptide vaccine + IFN-β or with IFN-β alone than in the other two groups. This indicates that IFN-β activated NK cells *in vivo*, and that the enhanced NK activity contributed to eradication of MHC class I-negative tumor cells or those with low MHC class I expression. Another merit was that MHC class I expression on the WT1-C1498 leukemia cells was enhanced. WT1 peptides were generated through intracellular processing of the WT1 protein in tumor cells and presented on the surface of these cells in association with MHC class I molecules, followed by the recognition of the WT1 peptide/MHC class I complex by WT1-specific CTLs. Consistent with previously reported findings [28,29], MHC-class I expression on the WT1-C1498 leukemia cells was enhanced in mice treated with WT1 peptide vaccine + IFN-β or IFN-β alone. Higher expression of MHC class I molecules contributes the recognition and attack by CTLs [29]. It is possible that in mice treated with WT1 peptide vaccine + IFN-β MHC class I expression on the WT1-C1498 leukemia cells was enhanced, resulting in a heightened vulnerability to attack by WT1-specific CTLs. Taken together, it seems likely that target cells (mWT1-C1498 cells), of which the MHC class I expression was enhanced by IFN-β, were efficiently killed by WT1-specific CTLs, while the remaining target cells with negative or low MHC class I expression were efficiently killed by NK cells whose activity was enhanced by IFN-β. IFN-α is another type I IFN and has the similar structure and function to IFN-β [31–36,45,47]. Furthermore, both IFN-α and IFN-β were approved for human use [30,37–40,48]. Therefore, it would be interesting to examine, using this experiment system, whether IFN-α, as well as IFN-β, is effective in the context of a combined use with WT1 peptide vaccine for the treatment of malignancies.

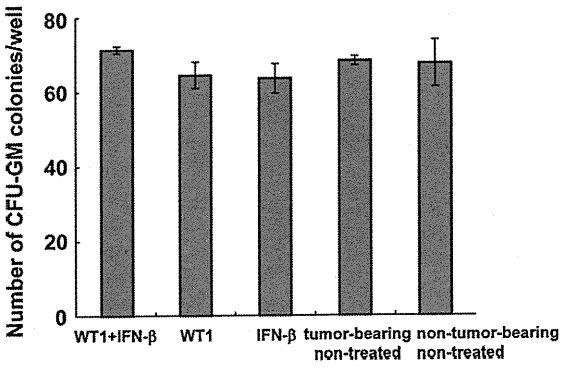

Fig. 6. No inhibition of colony-forming ability of bone marrow cells from mice immunized with WT1 peptide vaccine + IFN-β. Numbers of colonies generated by CFU-GM (colony-forming-unit granulocyte-macrophage) from mouse bone marrow cells on day 30. Values represent the means of the results from four mice in each group. Bars indicate standard errors.

Other functions of IFN-β in tumor rejection enhancement, that is, non-immunological mechanisms such as direct anti-tumor and anti-angiogenesis effect [32–34] may also have contributed to such rejection.

Although WT1 is physiologically expressed in some type of normal cells, including hematopoietic stem/progenitor cells and kidney glomeruli, WT1 vaccination combined with IFN-β treatment did not diminish the GM colony-forming ability of BM cells (Fig. 6), which is in agreement with previous reports [25,27]. These findings indicate that WT1-specific CTLs did not recognize normal cells that physiologically expressed *WT1*. The reason for this lack of recognition appears to be that WT1-specific CTLs can

discriminate only between *WT1*-expressing tumor cells and physiologically *WT1*-expressing normal cells, resulting in the selective killing of tumor cells with no damage to normal tissues. These results suggested that the mechanisms involved in processing of WT1 protein and/or presentation of WT1 peptide might be different between tumor and normal cells, resulting in no or weak presentation of the WT1 peptide on the cell surface of normal cells. Further studies to address this issue are clearly warranted.

Immunopotentiating agents play a key role in the success of cancer immunotherapy, because injection of CTL epitope peptide alone cannot sufficiently induce and activate the TAA-specific CTLs. Co-administration of CTL epitope peptides and immunopotentiating agents proved to be effective for induction and activation of the CTLs and/or activation of other effector cells such as NK cells. We previously reported that the WT1 peptide vaccine combined with *M. bovis* bacillus Calmette-Guérin cell wall skeleton (BCG-CWS), which activates DCs through TLRs 2 and 4, had a synergistic effect on tumor rejection in mice [27]. In the current study, we could demonstrate the immunopotentiating activities of IFN-β leading to the enhancement of WT1-specific CTLs, NK cells, and MHC class I expression. It is anticipated that WT1 peptide vaccination combined with both IFN-β and BCG-CWS will be more effective for tumor rejection. The combination of CTL epitope vaccine with some immunopotentiating agents with various mechanisms for enhancement of anti-tumor immunity can be expected to become part of effective strategies for the cancer immunotherapy. Clinical trials of WT1 peptide cancer vaccine have already been started, and WT1 peptide vaccination was shown to have good potential for the treatment of cancer [14–17,49–54]. So far, we have performed immunization using WT1 peptide with Montanide ISA 51 adjuvant, and another group used KLH and GM-CSF [55]. Since the safety and toxicity of IFN-β have been confirmed to a considerable extent [37–40], WT1 peptide vaccination combined with IFN-β should be ready for use in the clinical settings in the near future.

Acknowledgement

We would like to thank Ms. Sachie Mamitsuka-Watanabe for preparation of this manuscript.

References

[1] Call KM, Glaser T, Ito CY, Buckler AJ, Pelletier J, Haber DA, et al. Isolation and characterization of a zinc finger polypeptide gene at the human chromosome 11 Wilms' tumor locus. Cell 1990;60:509–20.
[2] Gessler M, Poustka A, Cavenee W, Nevel RL, Orkin SH, Bruns GAP. Homozygous deletion in Wilms tumors of a zinc-finger gene identified by chromosome jumping. Nature 1990;343:774–8.
[3] Menke AL, Van der Eb AJ, Jochemsen AG. The Wilms' tumor 1 gene: oncogene or tumor suppressor gene. Int Rev Cytol 1998;181:151–212.
[4] Inoue K, Sugiyama H, Ogawa H, Nakagawa M, Yamagami T, Miwa H, et al. WT1 as a new prognostic factor and a new marker for the detection of minimal residual disease in acute leukemia. Blood 1994;84:3071–9.
[5] Inoue K, Ogawa H, Sonoda Y, Kimura T, Sakabe H, Oka Y, et al. Aberrant overexpression of the Wilms' tumor gene (WT1) in human leukemia. Blood 1997;89:1405–12.
[6] Briegar J, Weidmann E, Fenchel K, Mitrou PS, Hoelzer D, Bergmann L. The expression of the Wilms' tumor gene in acute myelocytic leukemias as a possible marker for leukemic blast cells. Leukemia 1994;8:2138–43.
[7] Miwa H, Beran M, Saunders GF. Expression of the Wilms' tumor gene (WT1) in human leukemias. Leukemia 1992;6:405–9.
[8] Menssen HD, Renkl HJ, Rodeck U, Maurer J, Notter M, Schwartz S, et al. Presence of Wilms' tumor gene (WT1) transcripts and the WT1 nuclear protein in the majority of human acute leukemias. Leukemia 1995;9:1060–7.
[9] Oji Y, Ogawa H, Tamaki H, Oka Y, Tsuboi A, Kim EH, et al. Expression of the Wilms' tumor gene WT1 in solid tumors and its involvement in tumor cell growth. Jpn J Cancer Res 1999;90:194–204.
[10] Oji Y, Miyoshi S, Maeda H, Hayashi S, Tamaki H, Nakatsuka S, et al. Overexpression of the Wilms' tumor gene WT1 in de novo lung cancers. Int J Cancer 2002;100:297–303.
[11] Loeb DM, Evron E, Patel CB, Sharma PM, Niranjan B, Buluwela L, et al. Wilms' tumor suppressor gene (WT1) is expressed in primary breast tumors despite tumor-specific promotor methylation. Cancer Res 2001;61:921–5.
[12] Oji Y, Yamamoto H, Nomura M, Nakano Y, Ikeba A, Nakatsuka S, et al. Overexpression of the Wilms' tumor gene WT1 in colorectal adenocarcinoma. Cancer Sci 2003;94:712–7.
[13] Oji Y, Suzuki T, Nakano Y, Maruno M, Nakatsuka S, Jomgeow T, et al. Overexpression of the Wilms' tumor gene WT1 in primary astrocytic tumors. Cancer Sci 2004;95:822–7.
[14] Sugiyama H. Cancer immunotherapy targeting WT1 protein. Int J Hematol 2002;76:127–32.
[15] Sugiyama H. Cancer immunotherapy targeting Wilms' tumor gene WT1 product. Expert Rev Vaccines 2005;4:503–12.
[16] Oka Y, Tsuboi A, Kawakami M, Elisseeva OA, Nakajima H, Udaka K, et al. Development of WT1 peptide cancer vaccine against hematopoietic malignancies and solid cancers. Curr Med Chem 2006;13:2345–52.
[17] Oka Y, Tsuboi A, Elisseeva OA, Nakajima H, Fujiki F, Kawakami M, et al. WT1 peptide cancer vaccine for patients with hematopoietic malignancies and solid cancers. ScientificWorldJournal 2007;29:649–65.
[18] Yamagami T, Sugiyama H, Inoue K, Ogawa H, Tatekawa T, Hirata M, et al. Growth inhibition of human leukemic cells by WT1 (Wilms tumor gene) antisense oligonucleotides: implications for the involvement of WT1 in leukemogenesis. Blood 1996;87:2878–84.
[19] Inoue K, Tamaki H, Ogawa H, Oka Y, Soma T, Tatekawa T, et al. Wilms' tumor gene (WT1) competes with differentiation-inducing signal in hematopoietic progenitor cells. Blood 1998;91:2969–76.
[20] Tsuboi A, Oka Y, Ogawa H, Elisseeva OA, Tamaki H, Oji Y, et al. Constitutive expression of the Wilms' tumor gene WT1 inhibits the differentiation of myeloid progenitor cells but promotes their proliferation in response to granulocyte-colony stimulating factor (G-CSF). Leuk Res 1999;23:499–505.
[21] Oka Y, Elisseeva OA, Tsuboi A, Ogawa H, Tamaki H, Li H, et al. Human cytotoxic T-lymphocyte response specific for peptides of the wild-type Wilms' tumor gene (WT1) product. Immunogenetics 2000;51:99–107.
[22] Gao L, Bellantuono I, Elsässer A, Marley SB, Gordon MY, Goldman JM, et al. Selective elimination of leukemic CD34$^+$ progenitor cells by cytotoxic T lymphocytes specific for WT1. Blood 2000;95:2198–203.
[23] Ohminami H, Yasukawa M, Fujita S. HLA class I-restricted lysis of leukemia cells by a CD8$^+$ cytotoxic T-lymphocyte clone specific for WT1 peptide. Blood 2000;95:286–93.
[24] Oka Y, Udaka K, Tsuboi A, Elisseeva OA, Ogawa H, Aozasa K, et al. Cancer immunotherapy targeting Wilms' tumor gene WT1 product. J Immunol 2000;164:1873–80.
[25] Tsuboi A, Oka Y, Ogawa H, Elisseeva OA, Li H, Kawasaki K, et al. Cytotoxic T-lymphocyte responses elicited to Wilms' tumor gene WT1 product by DNA vaccination. J Clin Immunol 2000;20:195–202.
[26] Yasumoto K, Manabe H, Yanagawa E, Nagano N, Ueda H, Hirota N, et al. Non-specific adjuvant immunotherapy of lung cancer with cell wall skeleton of *Mycobacterium bovis* Bacillus Calmette-Guérin. Cancer Res 1979;39:3262–7.
[27] Nakajima H, Kawasaki K, Oka Y, Tsuboi A, Kawakami M, Ikegame K, et al. WT1 peptide vaccination combined with BCG-CWS is more efficient for tumor eradication than WT1 peptide vaccination alone. Cancer Immunol Immunother 2004;53:617–24.
[28] Dhib-Jalbut SS, Cowan EP. Direct evidence that interferon-β mediates enhanced HLA-Class I expression in measles virus-infected cells. J Immunol 1993;11:6248–58.
[29] Dezfouli S, Hatzinisiriou I, Ralph SJ. Enhancing CTL responses to melanoma cell vaccines in vivo: synergistic increases obtained using IFN-γ primed and IFN-β treated B7-1$^+$ B16-F10 melanoma cells. Immunol Cell Biol 2003;81:459–71.
[30] Kirkwood JM, Richards T, Zarour HM, Sosman J, Ernstoff M, Whiteside TL, et al. Immunomodulatory effects of high-dose and low-dose interferon α2b in patients with high-risk resected melanoma: the E2690 laboratory corollary of intergroup adjuvant trial E1690. Cancer 2002;95:1101–12.
[31] Kayagaki N, Yamaguchi N, Nakayama M, Eto H, Okumura K, Yagita H. Type I interferons (IFNs) regulate tumor necrosis factor-related apoptosis-inducing ligand (TRAIL) expression on human T cells: a novel mechanism for the antitumor effects of type I IFNs. J Exp Med 1999;189:1451–60.
[32] Tanabe T, Kominsky SL, Subramaniam PS, Johnson HM, Torres BA. Inhibition of the glioblastoma cell cycle by type I IFNs occurs at both the G1 and S phases and correlates with the upregulation of p21(WAF1/CIP1). J Neurooncol 2000;48:225–32.
[33] Chen Q, Gong B, Mahmoud-Ahmed AS, Zhou A, Hsi ED, Hussein M, et al. Apo2L/TRAIL and Bcl-2-related proteins regulate type I interferon-induced apoptosis in multiple myeloma. Blood 2001;98:2183–92.
[34] Streck CJ, Zhang Y, Miyamoto R, Zhou J, Ng CY, Nathwani AC, et al. Restriction of neuroblastoma angiogenesis and growth by interferon-α/β. Surgery 2004;136:183–9.
[35] Wakita D, Chamoto K, Zhang Y, Narita Y, Noguchi D, Ohnishi H, et al. An indispensable role of type-1 IFNs for inducing CTL-mediated complete eradication of established tumor tissue by CpG-liposome co-encapsulated with model tumor antigen. Int Immunol 2006;18:425–34.
[36] Gehring S, Gregory SH, Kuzushita N, Wands JR. Type 1 interferon augments DNA-based vaccination against hepatitis C virus core protein. J Med Virol 2005;75:249–57.
[37] Mani S, Todd M, Poo WJ. Recombinant beta-interferon in the treatment of patients with metastatic renal cell carcinoma. Am J Clin Oncol 1996;19:187–9.
[38] Fine HA, Wen PY, Robertson M, O'Neill A, Kowal J, Loeffler JS, et al. A phase I trial of a new recombinant human beta-interferon (BG9015) for the treatment of patients with recurrent gliomas. Clin Cancer Res 1997;3:381–7.

[39] Beppu T, Kamada K, Nakamura R, Oikawa H, Takeda M, Fukuda T, et al. A phase II study of radiotherapy after hyperbaric oxygenation combined with interferon-beta and nimustine hydrochloride to treat supratentorial malignant gliomas. J Neurooncol 2003;61:161–70.
[40] Watanabe T, Katayama Y, Yoshino A, Fukaya C, Yamamoto T. Human interferon beta, nimustine hydrochloride, and radiation therapy in the treatment of newly diagnosed malignant astrocytomas. J Neurooncol 2005;72:57–62.
[41] Yamaguchi S, Tatsumi T, Takehara T, Sakamori R, Uemura A, Mizushima T, et al. Immunotherapy of murine colon cancer using receptor tyrosine kinase EphA2-derived peptide-pulsed dendritic cell vaccines. Cancer 2007;110:1469–77.
[42] Degli-Esposti MA, Smyth MJ. Close encounters of different kinds: dendritic cells and NK cells take centre stage. Nat Rev Immunol 2005;5:112–24.
[43] Fedele G, Frasca L, Palazzo R, Ferrero E, Malavasi F, Ausiello CM. CD38 is expressed on human mature monocyte-derived dendritic cells and is functionally involved in CD83 expression and IL-12 induction. Eur J Immunol 2004;34:1342–50.
[44] He T, Tang C, Xu S, Moyana T, Xiang J. Interferon gamma stimulates cellular maturation of dendritic cell line DC2.4 leading to induction of efficient cytotoxic T cell responses and antitumor immunity. Cell Mol Immunol 2007;4:105–11.
[45] Sato K, Hida S, Takayanagi H, Yokochi T, Kayagaki N, Takeda K, et al. Antiviral response by natural killer cells through TRAIL gene induction by IFN-α/β. Eur J Immunol 2001;31:3138–46.
[46] Raghuraman G, Geng Y, Wang CR. IFN-β-mediated up-regulation of CD1d in bacteria-infected APCs. J Immunol 2006;177:7841–8.
[47] Gresser I. The antitumor effects of interferon: a personal history. Biochimie 2007;89:723–8.
[48] Anguille S, Lion E, Willemen Y, Van Tendeloo VF, Berneman ZN, Smits EL. Interferon-α in acute myeloid leukemia: an old drug revisited. Leukemia 2011;25:739–48.
[49] Oka Y, Tsuboi A, Murakami M, Hirai M, Tominaga N, Nakajima H, et al. Wilms tumor gene peptide-based immunotherapy for patients with overt leukemia from myelodysplastic syndrome (MDS) or MDS with myelofibrosis. Int J Hematol 2003;78:56–61.
[50] Tsuboi A, Oka Y, Osaki T, Kumagai T, Tachibana I, Hayashi S, et al. WT1 peptide-based immunotherapy for patients with lung cancer: report of two cases. Microbiol Immunol 2004;48:175–84.
[51] Oka Y, Tsuboi A, Taguchi T, Osaki T, Kyo T, Nakajima H, et al. Induction of WT1 (Wilms' tumor gene)-specific cytotoxic T lymphocytes by WT1 peptide vaccine and the resultant cancer regression. Proc Natl Acad Sci USA 2004;101:13885–90.
[52] Morita S, Oka Y, Tsuboi A, Kawakami M, Maruno M, Izumoto S, et al. A phase I/II trial of a WT1 (Wilms' tumor gene) peptide vaccine in patients with solid malignancy: safety assessment based on the phase I data. Jpn J Clin Oncol 2006;36:231–6.
[53] Kawakami M, Oka Y, Tsuboi A, Harada Y, Elisseeva OA, Furukawa Y, et al. Clinical and immunologic responses to very low-dose vaccination with WT1 peptide (5 μg/body) in a patient with chronic myelomonocytic leukemia. Int J Hematol 2007;85:426–9.
[54] Iiyama T, Udaka K, Takeda S, Takeuchi T, Adachi YC, Ohtsuki Y, et al. WT1 (Wilms' tumor 1) peptide immunotherapy for renal cell carcinoma. Microbiol Immunol 2007;51:519–30.
[55] Mailänder V, Scheibenbogen C, Thiel E, Letsch A, Blau IW, Keilholz U. Complete remission in a patient with recurrent acute myeloid leukemia induced by vaccination with WT1 peptide in the absence of hematological or renal toxicity. Leukemia 2004;18:165–6.

J Neurosurg 116:835–842, 2012

Use of ^{11}C-methionine PET parametric response map for monitoring WT1 immunotherapy response in recurrent malignant glioma

Clinical article

Yasuyoshi Chiba, M.D., Ph.D.,[1] Manabu Kinoshita, M.D., Ph.D.,[1] Yoshiko Okita, M.D., Ph.D.,[1] Akihiro Tsuboi, M.D., Ph.D.,[2] Kayako Isohashi, M.D., Ph.D.,[3] Naoki Kagawa, M.D., Ph.D.,[1] Yasunori Fujimoto, M.D., Ph.D.,[1] Yusuke Oji, M.D., Ph.D.,[4] Yoshihiro Oka, M.D., Ph.D.,[5] Eku Shimosegawa, M.D., Ph.D.,[3] Satoshi Morita, Ph.D.,[6] Jun Hatazawa, M.D., Ph.D.,[3] Haruo Sugiyama, M.D., Ph.D.,[7] Naoya Hashimoto, M.D., Ph.D.,[1] and Toshiki Yoshimine, M.D., Ph.D.[1]

Departments of [1]Neurosurgery; [2]Cancer Immunotherapy; [3]Nuclear Medicine and Tracer Kinetics; [4]Cancer Stem Cell Biology; [5]Respiratory Medicine, Allergy, and Rheumatic Diseases; and [7]Functional Diagnostic Science, Osaka University Graduate School of Medicine, Osaka; and [6]Department of Biostatistics and Epidemiology, Yokohama City University Graduate School of Medicine, Yokohama, Japan

Object. Immunotherapy targeting the *Wilms tumor 1 (WT1)* gene product is a promising treatment modality for patients with malignant gliomas, and there have been reports of encouraging results. It has become clear, however, that Gd-enhanced MR imaging does not reflect prognosis, thereby necessitating a more robust imaging evaluation system for monitoring response to WT1 immunotherapy. To meet this demand, the authors performed a voxel-wise parametric response map (PRM) analysis of ^{11}C-methionine PET (MET-PET) in WT1 immunotherapy and compared the data with the overall survival after initiation of WT1 immunotherapy (OS_{WT1}).

Methods. Fourteen patients with recurrent malignant glioma were included in the study, and OS_{WT1} was compared with: 1) volume and length change in the contrast area of the tumor on Gd-enhanced MR images; 2) change in maximum uptake of ^{11}C-methionine; and 3) a more detailed voxel-wise PRM analysis of MET-PET pre- and post-WT1 immunotherapy.

Results. The PRM analysis was able to identify the following 3 areas within the tumor core: 1) area with no change in ^{11}C-methionine uptake pre- and posttreatment; 2) area with increased ^{11}C-methionine uptake posttreatment (PRM^{+MET}); and 3) area with decreased ^{11}C-methionine uptake posttreatment. While the results of Gd-enhanced MR imaging volumetric and conventional MET-PET analysis did not correlate with OS_{WT1} ($p = 0.270$ for Gd-enhanced MR imaging length, $p = 0.960$ for Gd-enhanced MR imaging volume, and $p = 0.110$ for MET-PET), the percentage of PRM^{+MET} area showed excellent correlation ($p = 0.008$) with OS_{WT1}.

Conclusions. This study describes the limited value of Gd-enhanced MR imaging and highlights the potential of voxel-wise PRM analysis of MET-PET for monitoring treatment response in immunotherapy for malignant gliomas. Clinical trial registration no.: UMIN000002001.
(http://thejns.org/doi/abs/10.3171/2011.12.JNS111255)

Key Words • **glioma** • **^{11}C-methionine PET** • **WT1 immunotherapy** • **parametric response map** • **oncology**

Malignant glioma remains a devastating intracranial neoplasm. In particular, patients with newly diagnosed GBM have a median overall survival of only 14.6 months, even when treated with chemotherapeutic agents such as temozolomide.[17] On the other hand, the products of the *WT1* gene have been shown to be overexpressed in malignant gliomas,[12,13] and this makes the WT1 antigen an attractive target for immunotherapy against malignant glioma.

The results of WT1 immunotherapy have been previously reported for the initial 21 patients participating in an ongoing Phase II clinical trial of WT1 vaccination for patients with recurrent malignant glioma, and the safety and efficacy of WT1 vaccination have been described (Phase I/II clinical trial of WT1 peptide-based vaccine for the patients with malignant tumors. UMIN000002001).[9]

Abbreviations used in this paper: GBM = glioblastoma multiforme; MET-PET = ^{11}C-methionine PET; OS_{WT1} = overall survival after initiation of Wilms tumor 1 immunotherapy; PRM = parametric response map; RECIST = Response Evaluation Criteria in Solid Tumors; ROI = region of interest; WT1 = Wilms tumor 1.

This article contains some figures that are displayed in color online but in black and white in the print edition.

The median overall survival time after initiating WT1 immunotherapy was 36.7 weeks. In that report, the antitumor effect of the treatment was assessed by determining the response of the target lesions using MR imaging 12 weeks after initiating WT1 vaccination. The tumor length, corresponding to the contrast-enhanced area on Gd-enhanced MR images, was measured and analyzed according to RECIST version 1.0,[18] with results reported as complete response, partial response, stable disease, and progressive disease.

In that analysis, however, the long-term survivors were assessed as having progressive disease at 12 weeks after WT1 vaccination initiation, suggesting that evaluation by contrast-enhanced T1-weighted MR imaging is not suitable for assessing the treatment response to WT1 immunotherapy. The fact that morphological imaging often does not adequately reflect the underlying tumor biology[3] imposes a considerable demand to develop alternative biological markers for therapeutic response. Recently, a voxel-wise PRM has been developed to overcome the above-mentioned issue in other treatment modalities for malignant glioma.[6–8]

The present report focuses on the results in 14 patients who were enrolled in the same trial but were not included in the previous report. In this study, we have attempted to apply the voxel-wise PRM method to MET-PET in the setting of WT1 immunotherapy against recurrent malignant glioma and compare its clinical value with conventional analytical methods based on MR imaging and PET.

Methods

WT1 Immunotherapy

Patients received intradermal injections of 3.0 mg of modified 9-mer WT1 peptide emulsified with Montanide ISA51 adjuvant. The WT1 vaccinations were given weekly for 12 consecutive weeks. Twelve weeks after the initial vaccination, the response was evaluated by means of both MR imaging and MET-PET. Our local internal review board approved this treatment and written informed consent was obtained from all patients. Details of the procedures and protocol have been reported elsewhere.[9,14]

Patient Selection

Between 2004 and 2010, 66 patients with recurrent malignant glioma were treated with WT1 immunotherapy as described above as part of an ongoing clinical trial (UMIN000002001). Nineteen of these 66 patients underwent evaluation by means of MET-PET. These patients were not included in our previous report.[9] Five of these 19 patients—2 patients with intratumoral hematoma and 3 patients whose tumor volume was 2 cm^3 or less as measured by MET-PET—were excluded from the current analysis. All 14 patients whose data were analyzed for this study underwent MR imaging and MET-PET before (pre-WT1) and 12 weeks after (post-WT1) WT1 vaccination. Detailed information pertaining to these 14 patients is listed in Table 1. The overall survival was measured from WT1 immunotherapy initiation, denoted as OS_{WT1}.

Magnetic Resonance Imaging

All MR images were obtained using a 3.0-T whole-body MR scanner (Signa, GE Medical Systems) with an acquisition time of approximately 3 minutes. After intravenous administration of Gd–diethylenetriamine pentaacetic acid (Gd-DTPA; 0.1 mmol/kg body weight), axial T1-weighted images were obtained using standard procedures. Those images were stored in 512 × 512 × 23 or 216 anisotropic voxels, with each voxel being 0.43 × 0.43 × 6.0 or 1.0 mm.

MET-PET Scans

All PET studies were performed using the Eminence PET system (Shimadzu Corp.). ^{11}C-methionine (111–222 MBq, 3–6 mCi), synthesized according to the method of Berger et al.,[1] was injected intravenously. Tracer accumulation was recorded over 15 minutes in 99 transaxial slices from the entire brain. Total activity from 20 to 35 minutes after tracer injection was used for image reconstruction. The images were stored in 256 × 256 × 99 anisotropic voxels, with each voxel being 1 × 1 × 2.6 mm.

Tumor Length and Volume Measurement

Tumor length, corresponding to the contrast-enhanced area on T1-weighted MR images, was measured and analyzed according to RECIST version 1.0,[18] using the ImageJ software from the National Institutes of Health (http://rsb.info.nih.gov/ij/).

Tumor volume was measured by performing a 3D threshold-based volume-of-interest analysis in all patients for contrast-enhanced lesions on Gd-enhanced MR images, using the ImageJ software. The contrast-enhanced area in each slice image was measured by manual tracking of the tumor boundaries, and the sum of the enhanced areas or high-uptake areas was multiplied by the slice interval.

Image Fusion and Registration

The MET-PET data were registered onto pre-WT1 contrast-enhanced T1-weighted standard anatomical images using normalized mutual information with the VINCI image analyzing software from the Max Planck Institute for Neurological Research in Cologne (http://www.nf.mpg.de/vinci/). Registration of the images was confirmed visually. The reported registration error for normalized mutual information is less than 1 mm.[19] After image registration was completed, all image sets, including the standard anatomical MR images (pre-WT1) and MET-PET data (pre- and post-WT1), were converted into 256 × 256 × 256 isotropic, 1 × 1 × 1 mm images enabling further voxel-wise analysis of the images (Fig. 1).

Data Processing and ROI Selection

Three data sets (standard anatomical images and MET-PET data) were exported to in-house software written in MATLAB 7.6 (MathWorks) for further analysis. Regions of interest were selected as follows: for normal brain tissue, the contralateral hemisphere of the tumor was selected, including both the gray and white matter; for tumor, contrast-enhanced lesions were selected.

TABLE 1: Summary of clinical and demographic characteristics of 14 patients*

Case No.	Age (yrs),† Sex	ECOG PS	Diagnosis	Response per RECIST	OS_{WT1} (wks)‡	Tumor Vol by MET-PET (cm^3)§
1	43, M	2	GBM	SD	87.1	31.2
2	64, M	1	GBM	PD	144.7	63.8
3	76, M	1	GBM	SD	144.6	29
4	60, F	0	GBM	SD	61.7	58.1
5	20, F	0	GBM	PR	29.3	24.9
6	64, F	1	AA	SD	65.0	51
7	29, M	2	GBM	PD	20.9	15.4
8	28, M	1	GBM	SD	57.7	9
9¶	62, M	0	gliosarcoma	SD	77.0	11.5
10	36, F	1	AA	SD	60.3	3.8
11	44, M	0	GBM	PD	48.1	13.2
12	62, F	1	GBM	PD	18.7	5
13	51, M	0	GBM	PD	35.0	39.3
14	39, F	1	GBM	PD	27.6	15.2

* AA = anaplastic astrocytoma; ECOG PS = Eastern Cooperative Oncology Group Performance Status; PD = progressive disease; PR = partial response; SD = stable disease.
† Mean 48.4 years.
‡ Median 59.0 weeks.
§ Median 26.5 cm^3.
¶ The patient in Case 9 was alive as of this writing.

Parametric Response Map Calculation Algorithm

As in Fig. 1, post-WT1 ^{11}C-methionine uptake was plotted as a function of pre-WT1 ^{11}C-methionine uptake in both normal brain and Gd-enhancing lesions. A linear regression fitting was applied to the data obtained by the ROI placed at the normal brain (Fig. 1, *blue line*), which can be expressed as follows: post-WT1 MET-PET = pre-WT1 MET-PET, where "post-WT1 MET-PET" and "pre-WT1 MET-PET" are the tumor/normal tissue (T/N) ratio of pre- and post-WT1 ^{11}C-methionine PET.

Next, the magnitude of deviation of each data point *(i)* from the expected linear regression fitting was calculated as follows:

$$\text{deviation}_i = [(\text{post-WT1 MET-PET})_i - (\text{pre-WT1 MET-PET})_i] / \sqrt{2}$$

The parametric response map (PRM) of each data point was defined as follows:

$$PRM_i = \text{deviation}_i - \mu / \rho$$

where μ and ρ are the mean and standard deviation of deviation_i within the ROI placed at the normal brain. In other words, PRM is identical to the z-score of each data point in the lesion from the expected linear regression line calculated for normal brain.

Statistical Analysis

Statistical analyses were carried out using a Kaplan-Meyer survival analysis with the log-rank test if not specified otherwise. A p value < 0.05 was considered statistically significant, and all statistical computation was performed using Prism 5 (GraphPad Software, Inc.) or JMP 9.0 (SAS Institute, Inc.).

Results

Applying the PRM Calculation to WT1 Immunotherapy Patients

The PRM calculation, described above and in Fig. 1, was successfully performed in all 14 cases. The actual process that was performed is described below by presenting 2 representative cases, one (Case 2) in which the patient had a relatively long OS_{WT1} of 144.7 weeks and was considered a treatment responder, and another (Case 7) in which the patient had a relatively short OS_{WT1} of 20.9 weeks and was considered a treatment nonresponder.

Representative Treatment Responder. A representative case involving a treatment responder (Case 2) is illustrated in Fig. 2. First, a voxel-wise analysis was performed in normal brain tissue (Figs. 1 and 2). As shown in Fig. 2, pre- and post-WT1 ^{11}C-methionine uptake showed good positive linear correlation in normal brain tissue. A linear regression line and the ± 2 SD distribution range were calculated. Subsequently, the same analysis was performed in a tumor lesion. A contrast-enhanced area was selected as the ROI for analysis. In this particular case, most voxels were distributed in the –2 SD area, suggesting that ^{11}C-methionine uptake decreased after WT1 immunotherapy (Fig. 2). This area is presented as PRM^{-MET} (PRM with reduced methionine uptake).

This patient survived for 144.7 weeks after initiation of WT1 immunotherapy, although the contrast-enhanced area increased after WT1 immunotherapy, categorizing this patient as having progressive disease in the Gd-enhanced MR imaging–based RECIST analysis.

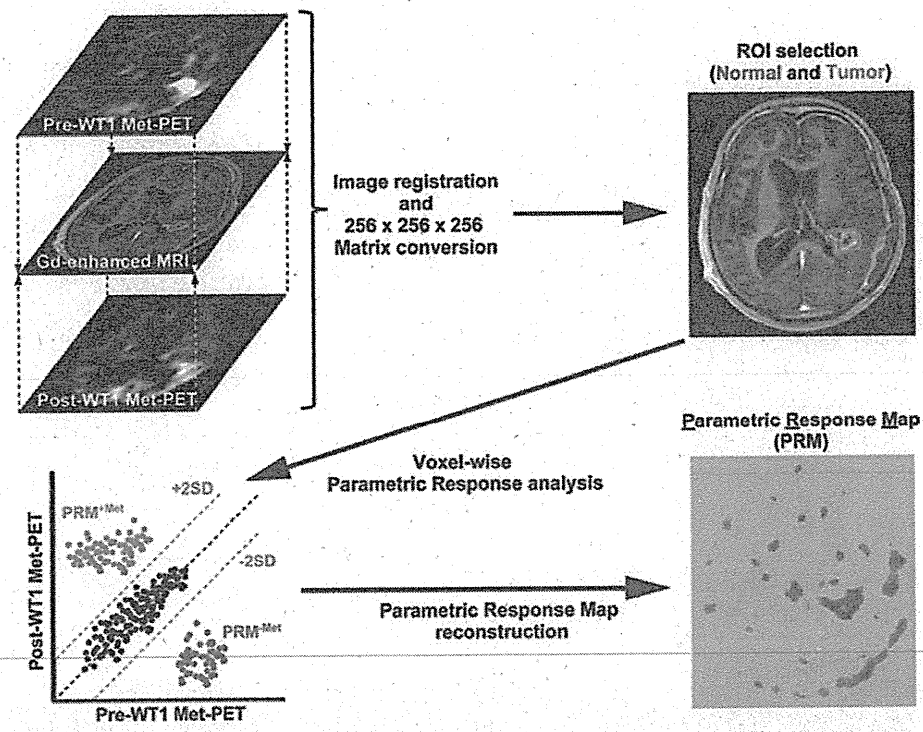

FIG. 1. Image processing procedures. ^{11}C-methionine PET data obtained before and 12 weeks after WT1 immunotherapy initiation were fused and registered onto conventional contrast-enhanced MR images. All 3 images were converted into a 256 × 256 × 256, 1-mm isotropic image matrix. Post-WT1 ^{11}C-methionine uptake was plotted as a function of pre-WT1 ^{11}C-methionine uptake. After calculating the linear regression line with the ± 2 SD distribution range in contralateral normal brain tissue, an ROI was set at the contrast-enhanced pre-WT1 immunotherapy lesion. The obtained plots were categorized into the following 3 areas: 1) area of no change in ^{11}C-methionine uptake pre- and posttreatment, 2) area with increased ^{11}C-methionine uptake posttreatment (PRM^{+MET}), and 3) area with decreased ^{11}C-methionine uptake posttreatment (PRM^{-MET}). These areas were reconstructed in images for visual inspection (PRM^{+MET} in *red* and PRM^{-MET} in *blue*).

Representative Treatment Nonresponder. A representative case in which the patient had only a short OS_{WT1} (Case 7) is illustrated in Fig. 3. The same analysis as described above was performed. In this particular case, most voxels were distributed in the +2 SD area (PRM with increased methionine uptake [PRM^{+MET}]), suggesting that ^{11}C-methionine uptake increased after WT1 immunotherapy. This patient survived for 20.9 weeks after initiation of WT1 immunotherapy.

Correlation of Treatment Response Assessment and OS_{WT1}

Magnetic Resonance Imaging–Based Assessment. To assess the validity of evaluating the response to WT1 immunotherapy using contrast-enhanced MR imaging, the changes in length and volume of the tumor before and 12 weeks after initiating WT1 immunotherapy were calculated. As in Fig. 4A and B, both methods using Gd-enhanced MR imaging failed to show positive correlation with OS_{WT1} ($p = 0.270$ and 0.960, respectively).

Conventional MET-PET Analysis. To assess the validity of evaluating the response to WT1 immunotherapy using MET-PET, the changes in maximum ^{11}C-methionine uptake assessed using the tumor/normal tissue ratio (T/N max) before and 12 weeks after initiating WT1 immunotherapy were calculated. Change of T/N max failed to show any statistically significant correlation with OS_{WT1} ($p = 0.110$) (Fig. 4C).

Parametric Response Map Analysis. Finally, correlation of the proposed voxel-wise PRM of MET-PET with OS_{WT1} was investigated. Each voxel of contrast-enhanced area on the pretreatment MR images was categorized as a no-change area, PRM^{+MET}, or PRM^{-MET}, according to no change, increase, or decrease, respectively, in methionine uptake 12 weeks after initiation of WT1 immunotherapy. The percentage of the 3 categories was calculated 3-dimensionally and correlated with OS_{WT1} (Fig. 5). While the percentage of the PRM^{-MET} area showed moderate correlation with OS_{WT1} ($p = 0.100$) (Fig. 5 left), the percentage of the PRM^{+MET} area showed excellent correlation with OS_{WT1} ($p = 0.008$) (Fig. 5 right). A threshold of 5% for PRM^{+MET} yielded the best performance for discriminating WT1 immunotherapy responders from nonresponders (Fig. 5 right). When a Cox proportional hazard model was applied, adjusted by age (cutoff 50 years of age) and performance status (0 or 1 and 2), a threshold of 5% for PRM^{+MET} still remained as the only statistically significant factor ($p = 0.01$).

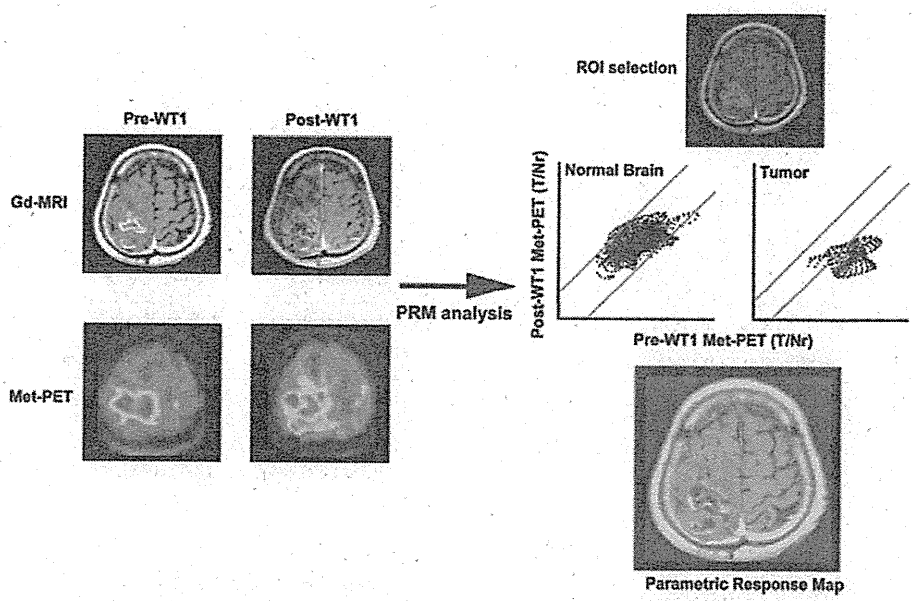

FIG. 2. Case 2. A representative treatment responder with recurrent GBM (OS_{WT1} 144.7 weeks). Images were analyzed as in Fig. 1. Voxel-wise PRM analysis revealed that most of the contrast-enhanced lesion was within the PRM^{-MET} area. Although the OS_{WT1} was 144.7 weeks, conventional MR imaging evaluated the response as progressive disease. Gd-MRI = Gd-enhanced MR imaging; T/Nr = T/N max.

Discussion

Conventionally, MR imaging is used to evaluate response to treatment in glioma patients. The maximum length of the contrast-enhanced area is measured and the effect of treatment is analyzed according to RECIST. This method is based on previous reports showing RECIST to be useful in determining objective responses of contrast-enhancing brain tumors to therapy. Moreover, those reports showed that use of RECIST was comparable to volumetric methods.[5,16] On the other hand, problems with using MR imaging–based tumor measurement as an indicator of treatment response have been reported. For example, temozolomide-based chemoradiotherapy for

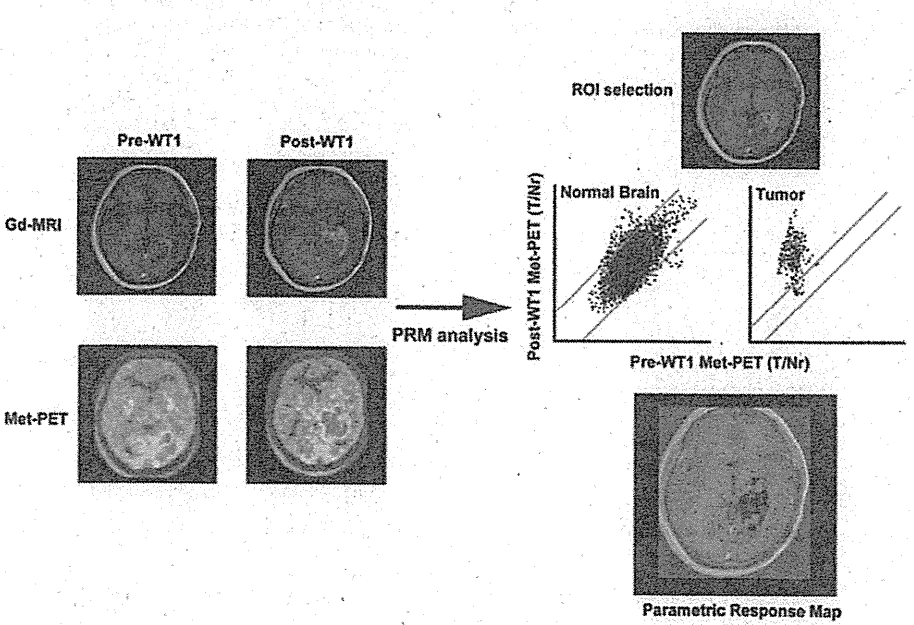

FIG. 3. Case 7. A representative treatment nonresponder with recurrent GBM (OS_{WT1} 20.9 weeks). Images were analyzed as in Fig. 1. Voxel-wise PRM analysis revealed that most of the contrast-enhanced lesion was within the PRM^{+MET} area, suggesting that the patient was not responsive to WT1 immunotherapy.

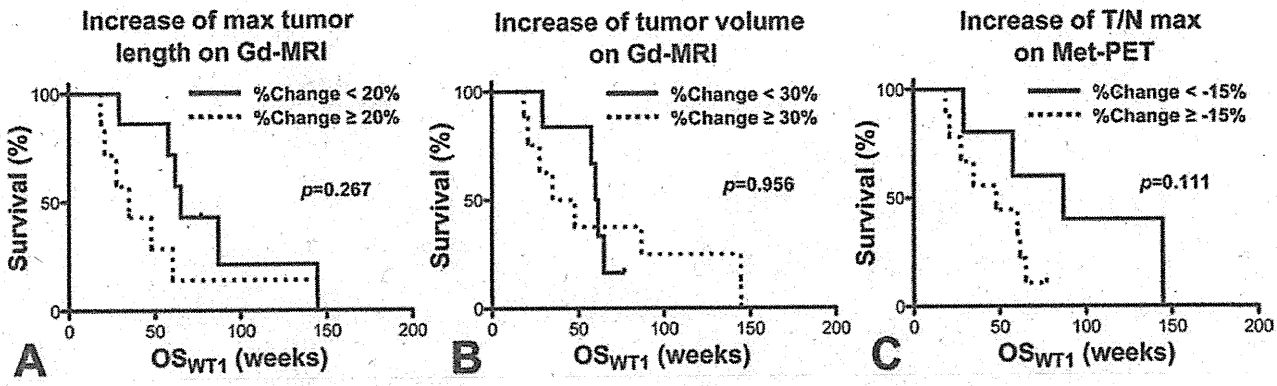

FIG. 4. Correlation of OS_{WT1} with changes in tumor length and volume using contrast-enhanced MR imaging and the T/N max of MET-PET. Correlations between OS_{WT1} and changes (from before WT1 immunotherapy to 12 weeks after immunotherapy initiation) on Gd-enhanced MR imaging–measured tumor length (**A**), volume (**B**), and T/N max of MET-PET (**C**) are presented. The correlations were not statistically significant (p = 0.270, 0.960, and 0.110, respectively; 14 cases).

newly diagnosed GBM results in a transient increase in tumor enhancement on MR imaging in 20%–30% of patients (pseudoprogression), which is difficult to differentiate from true tumor progression.[2] Similarly, in the present study, changes in tumor length and volume measured by contrast-enhanced MR imaging after WT1 immunotherapy did not correlate with OS_{WT1} (Fig. 4), suggesting that contrast-enhanced MR imaging is inappropriate for evaluating the clinical outcome of WT1 immunotherapy. Unlike chemotherapy or radiotherapy, immunotherapy causes an inflammatory reaction in the tumor, which results in infiltration of inflammatory cells, dilation of capillary vessels, and increased capillary permeability. Thus, it is possible that contrast enhancement does not reflect the tumor activity but rather represents the immune reaction in situ.

On the other hand, MET-PET provides high-resolution metabolic information about the tumor in vivo,[10] information that is impossible to obtain using MR imaging. Previous studies have shown that the ratio of the maximum ^{11}C-methionine uptake in tumor compared with the contralateral normal brain (T/N max) reflects prognosis.[4,11] However, gliomas are heterogeneous in nature and have heterogeneous uptake of ^{11}C-methionine. In fact, we have previously demonstrated that ^{11}C-methionine uptake correlates with tumor cell density by comparing MET-PET images with stereotactically sampled tissue.[15] Thus, instead of analyzing T/N max, which could result in comparisons between different locations within the tumor, a better method is to analyze the change in ^{11}C-methionine uptake in each anatomical location to elucidate the global change in ^{11}C-methionine uptake within the tumor. To satisfy this need, a voxel-wise PRM analysis[6–8] was used in the present study and produced excellent correlation between OS_{WT1} and the percentage of PRM^{+MET} (Fig. 5). This method showed far better correlation with OS_{WT1} than changes in T/N max by MET-PET, suggesting that the voxel-wise PRM is the most suitable method for assessing the treatment response of gliomas. Moreover, although the number of cases analyzed was small, a threshold of 5% for PRM^{+MET} was the best indicator for discriminating WT1 immunotherapy responders from nonresponders in terms of survival time (Fig. 5 right). A similar method has already been applied for diffusion or perfusion MR im-

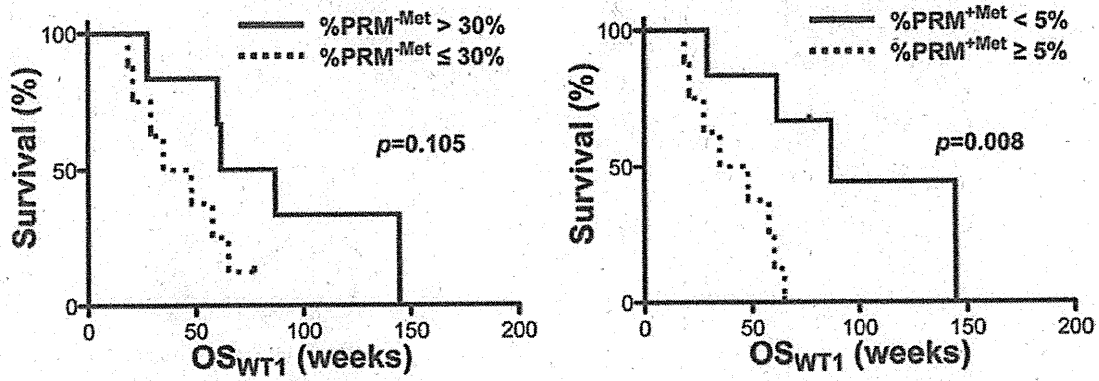

FIG. 5. Correlation of OS_{WT1} with PRM^{-MET} and PRM^{+MET}. Correlations between OS_{WT1} and percentage areas of PRM^{-MET} (**left**) and PRM^{+MET} (**right**) are presented. The percentage of PRM^{+MET} within the contrast-enhanced lesion before WT1 immunotherapy initiation correlated best with OS_{WT1} (p = 0.008; 14 cases).

aging analysis in glioma treatment using temozolomide and radiation therapy and has been suggested as an early biomarker for treatment response.[6–8] The main difference between voxel-wise PRM analysis and conventional imaging analysis is that voxel-wise PRM analysis allows us to identify the location and extent of areas that responded to therapy, rather than comparing the maximum values of the pre- and posttreatment evaluation modality, which could be comparing different locations.

There are, however, limitations that should be noted. Because pre- and posttreatment ^{11}C-methionine uptake is registered and compared, this method cannot be used when the shape or size dramatically change during therapy due to cyst formation or intratumoral hemorrhage. A more advanced method that could correct for tissue deformation is required to compensate for these changes. As the images compared were obtained 12 weeks apart, it is necessary to investigate the possibility of comparing images obtained in shorter intervals. Another limitation of this study is the retrospective nature of the data analysis and the limited sample size. Although a 5% cutoff of PRM^{+MET} yields the best result for the survival analysis, a prospective study with a much larger sample size will be necessary to obtain the most suitable cutoff value. Moreover, other modalities, such as perfusion or diffusion MR images should also be investigated in a similar manner to elucidate whether these modalities could also be used for evaluating immunotherapy for malignant gliomas.

Conclusions

We performed a voxel-wise PRM analysis of MET-PET before and 12 weeks after WT1 immunotherapy initiation to evaluate the clinical responses to WT1 immunotherapy in recurrent malignant glioma patients. This method holds promise for evaluating the dynamics of immunotherapy, which can be difficult to assess using conventional Gd-enhanced MR imaging.

Disclosure

The authors report no conflict of interest concerning the materials or methods used in this study or the findings specified in this paper. This work was supported in part by grants to Dr. Kinoshita from the Osaka Cancer Research Foundation, the Konica Minolta Imaging Science Foundation, the Osaka Cancer Researcher Training Fund, the Takeda Science Foundation, the Sagawa Foundation for Promotion of Cancer Research, and the Ministry of Education, Science and Culture of Japan, and by grants to Drs. Chiba and Hashimoto from the Ministry of Education, Science and Culture of Japan.

Author contributions to the study and manuscript preparation include the following. Conception and design: Kinoshita, Chiba, Tsuboi, Hashimoto, Yoshimine. Acquisition of data: Kinoshita, Chiba, Okita, Tsuboi, Isohashi, Kagawa, Fujimoto, Oji, Oka, Shimosegawa, Hatazawa, Hashimoto, Yoshimine. Analysis and interpretation of data: all authors. Drafting the article: Kinoshita, Chiba, Okita, Morita, Hashimoto, Yoshimine. Critically revising the article: all authors. Reviewed submitted version of manuscript: all authors. Approved the final version of the manuscript on behalf of all authors: Kinoshita. Statistical analysis: Kinoshita. Administrative/technical/material support: Tsuboi, Hashimoto, Yoshimine. Study supervision: Tsuboi, Oji, Oka, Hatazawa, Hashimoto, Yoshimine.

Acknowledgment

The authors thank Ms. Mariko Kakinoki (Department of Neurosurgery, Osaka University Graduate School of Medicine) for her assistance in the preparation of this manuscript.

References

1. Berger G, Maziere M, Knipper R, Prenant C, Comar D: Automated synthesis of 11C-labelled radiopharmaceuticals: imipramine, chlorpromazine, nicotine and methionine. **Int J Appl Radiat Isot 30:**393–399, 1979
2. Brandsma D, Stalpers L, Taal W, Sminia P, van den Bent MJ: Clinical features, mechanisms, and management of pseudoprogression in malignant gliomas. **Lancet Oncol 9:**453–461, 2008
3. Brasch R, Pham C, Shames D, Roberts T, van Dijke K, van Bruggen N, et al: Assessing tumor angiogenesis using macromolecular MR imaging contrast media. **J Magn Reson Imaging 7:**68–74, 1997
4. De Witte O, Goldberg I, Wikler D, Rorive S, Damhaut P, Monclus M, et al: Positron emission tomography with injection of methionine as a prognostic factor in glioma. **J Neurosurg 95:** 746–750, 2001
5. Galanis E, Buckner JC, Maurer MJ, Sykora R, Castillo R, Ballman KV, et al: Validation of neuroradiologic response assessment in gliomas: measurement by RECIST, two-dimensional, computer-assisted tumor area, and computer-assisted tumor volume methods. **Neuro Oncol 8:**156–165, 2006
6. Galbán CJ, Chenevert TL, Meyer CR, Tsien C, Lawrence TS, Hamstra DA, et al: The parametric response map is an imaging biomarker for early cancer treatment outcome. **Nat Med 15:**572–576, 2009
7. Galbán CJ, Chenevert TL, Meyer CR, Tsien C, Lawrence TS, Hamstra DA, et al: Prospective analysis of parametric response map-derived MRI biomarkers: identification of early and distinct glioma response patterns not predicted by standard radiographic assessment. **Clin Cancer Res 17:**7451–4760, 2011
8. Hamstra DA, Chenevert TL, Moffat BA, Johnson TD, Meyer CR, Mukherji SK, et al: Evaluation of the functional diffusion map as an early biomarker of time-to-progression and overall survival in high-grade glioma. **Proc Natl Acad Sci U S A 102:**16759–16764, 2005
9. Izumoto S, Tsuboi A, Oka Y, Suzuki T, Hashiba T, Kagawa N, et al: Phase II clinical trial of Wilms tumor 1 peptide vaccination for patients with recurrent glioblastoma multiforme. **J Neurosurg 108:**963–971, 2008
10. Jager PL, Vaalburg W, Pruim J, de Vries EG, Langen KJ, Piers DA: Radiolabeled amino acids: basic aspects and clinical applications in oncology. **J Nucl Med 42:**432–445, 2001
11. Nariai T, Tanaka Y, Wakimoto H, Aoyagi M, Tamaki M, Ishiwata K, et al: Usefulness of L-[methyl-11C] methionine-positron emission tomography as a biological monitoring tool in the treatment of glioma. **J Neurosurg 103:**498–507, 2005
12. Oji Y, Ogawa H, Tamaki H, Oka Y, Tsuboi A, Kim EH, et al: Expression of the Wilms' tumor gene WT1 in solid tumors and its involvement in tumor cell growth. **Jpn J Cancer Res 90:**194–204, 1999
13. Oji Y, Suzuki T, Nakano Y, Maruno M, Nakatsuka S, Jomgeow T, et al: Overexpression of the Wilms' tumor gene W T1 in primary astrocytic tumors. **Cancer Sci 95:**822–827, 2004
14. Oka Y, Tsuboi A, Taguchi T, Osaki T, Kyo T, Nakajima H, et al: Induction of WT1 (Wilms' tumor gene)-specific cytotoxic T lymphocytes by WT1 peptide vaccine and the resultant cancer regression. **Proc Natl Acad Sci U S A 101:**13885–13890, 2004
15. Okita Y, Kinoshita M, Goto T, Kagawa N, Kishima H, Shi-